FRONTIERS OF PHYSICS

TOPICAL REVIEW
Volume 21 / Issue 7 / 075302 / 2026

Altermagnetic ferrovalley materials: Paradigm shift and frontier advances in valleytronics

Yun-Qin Li [1,2], Wen-Yi Tong [1,2,†], Chun-Gang Duan [1,3,‡]

1 Key Laboratory of Polar Materials and Devices (MOE), School of Physics and Electronic Science and Shanghai Center of Brain-inspired Intelligent Materials and Devices, East China Normal University, Shanghai 200241, China
2 Suzhou National Laboratory, Suzhou 215123, China
3 Collaborative Innovation Center of Extreme Optics, Shanxi University, Taiyuan 030006, China
Corresponding authors. E-mail: †wytong@ee.ecnu.edu.cn, ‡cgduan@clpm.ecnu.edu.cn
Received December 22, 2025; accepted April 3, 2026

ABSTRACT

Valley degree of freedom, an intrinsic property of electrons, provides a novel dimension for information storage and processing. For most conventional valleytronic materials, however, stable and tunable valley polarization (VP) is usually realized based on spin–orbit coupling (SOC), which significantly limits material choices and operational flexibility. Altermagnetism — a novel magnetic order characterized by compensated magnetic order with vanishing net magnetization, broken inversion symmetry, and momentum-dependent spin splitting — offers a revolutionary solution to overcome this bottleneck. Originating from the coupling of altermagnetism and ferrovalley (FV) physics, the altermagnetic ferrovalley (AMFV) materials enable robust, tunable, and spontaneous spin-valley locking independently of strong SOC. This review systematically outlines the advances in AMFV materials. It begins by revisiting the types and limitations of traditional FV systems, then delves into the physical nature of altermagnetism and the symmetry principles underlying its integration with valley physics. Subsequently, it categorizes and reviews the latest theoretical and experimental progress on representative AMFV materials (e.g., V_2Se_2O, Fe_2MX_4), focusing on elucidating their multi-degree-of-freedom coupling characteristics (such as spin-valley-optical coupling) and their modulation mechanisms under external stimuli, including strain, electric field, sliding, twisting, and proximity effects. These AMFV systems hold enormous application potential in valley tunnel junctions and non-volatile memory, yet they still face challenges such as material scarcity, unclear mechanisms, and a lack of device-level exploration. Future efforts should leverage the synergy of high-throughput computation, advanced characterization techniques, and device development to drive breakthroughs and accelerate the development of next-generation information technologies.

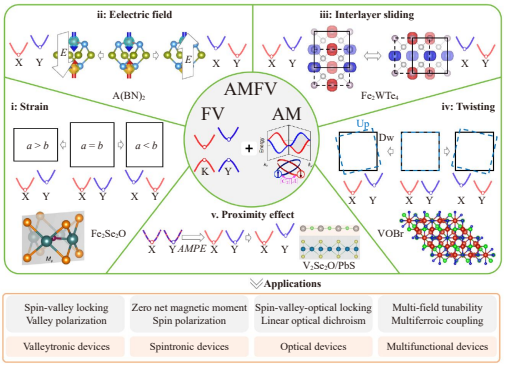

Keywords altermagnetism, ferrovalley materials, altermagnetic ferrovalley materials, valleytronics, spin-valley locking, multiferroic coupling

*Special Topic: Altermagnets: Exploring New Physical Phenomena and Effects (Editor: Sandong Guo).

Higher Education Press

https://doi.org/10.15302/frontphys.2026.075302

Contents

1 Introduction

The development of valleytronics stems from the in-depth exploration of the valley, an intrinsic degree of freedom of electrons [1–6]. Since the discovery of graphene in 2004, the exploration of its valley degree of freedom has gradually attracted widespread attention [7]. As band extrema of Bloch electrons in momentum space, valleys serve as stable binary information carriers, offering a new dimension for information encoding and storage [8–12]. In 2012, experimental verification of the valley Hall effect (VHE) and valley-dependent optical selection rules in monolayer MoS_2 marked the entry of valleytronics into experimental research [13–15]. Early studies mainly relied on external fields such as photoexcitation, magnetic field to induce VP, resulting in volatility in device information [16, 17]. In 2016, the concept of FV was formally proposed [18]. The coexistence of SOC and intrinsic magnetic exchange interaction can spontaneously break valley degeneracy, enabling stable valley polarization (VP) without external fields and laying the groundwork for nonvolatile valley devices [19–25]. Subsequently, ferroelectric ferrovalley (FV) materials (e.g., monolayer GeSe) were shown to generate tunable VP during ferroelectric switching, broadening the scope of FV research [26]. In recent years, FV physics has been discovered in various lattice systems, yielding rich multiferroic couplings with ferromagnetism and ferroelectricity (FE) [27–35]. Notably, recent studies have revealed that, contrary to traditional theoretical cognition, intrinsic FV behaviors can even exist in 2D bilayer systems with both time (T) and space (P) inversion symmetry, with VP switchable via ferroelasticity (FA) [36, 37]. Despite ongoing progress, VP modulation mostly relies on a single external field (e.g., electric field or strain) and generally depends on strong SOC. These limitations lead to insufficient modulation flexibility and a limited range of application material systems, which greatly hinder the development of high-performance and scalable valleytronic devices. The emergence of altermagnetism provides a promising pathway to overcome these bottlenecks.

As a magnetic order beyond the traditional ferromagnets (FM) and antiferromagnets (AFM) dichotomy, altermagnets (AM) exhibit zero net magnetic moment in real space but show significant non-relativistic spin splitting in momentum space [38, 39]. Crucially, their spin splitting originates from the broken PT symmetry rather than from strong SOC, opening up new opportunities for exploring spin and valley physics beyond heavy elements systems [40–45]. In recent years, altermagnetism has not only been experimentally confirmed in bulk materials such as CrSb, RuO_2, MnTe, and $Rb_{1-\delta}V_2Te_2O$ via spin-polarized angle-resolved photoemission spectroscopy (ARPES) [46–52], but also shows rich tunability in the two-dimensional (2D) limits [53–56]. The convergence of altermagnetism and FV physics has spawned the emerging field of AMFV materials. In 2021, spin-valley locking protected by crystal symmetry was first discovered in systems such as V_2Se_2O, where strain alone can induce and regulate large VP, overcoming the traditional reliance on strong SOC in FV materials [57]. Since then, theoretical progress has advanced in tandem with experimental breakthrough in altermagnetism: synergistic piezoelectric, piezomagnetic, and piezovalley effects were demonstrated in V_2SeTeO [58]; an electric field-tunable VP state was proposed in layered $A(BN)_2$ materials [59]; spin-valley-optical triple locking was found in the Fe_2MX_4 system [60]; a new sliding engineering approach for modulation of VP in AMFV was developed.

Although valleytronics and altermagnetism have been reviewed separately, existing reviews focus either on conventional SOC-dependent FV materials or on magnetic and spintronic properties, neglecting valley physics and device applications. To date, no review has systematically summarized the rapidly advancing AMFV field, particularly the spin-valley locking independent of SOC, unified material design principles, and multi-degree-of-freedom coupling mechanisms driven by altermagnetic order. This review fills this critical gap. Overall, AMFV materials mark a pivotal shift in valleytronics. They enable VP control through magnetic order and symmetry engineering, thus eliminating the reliance on

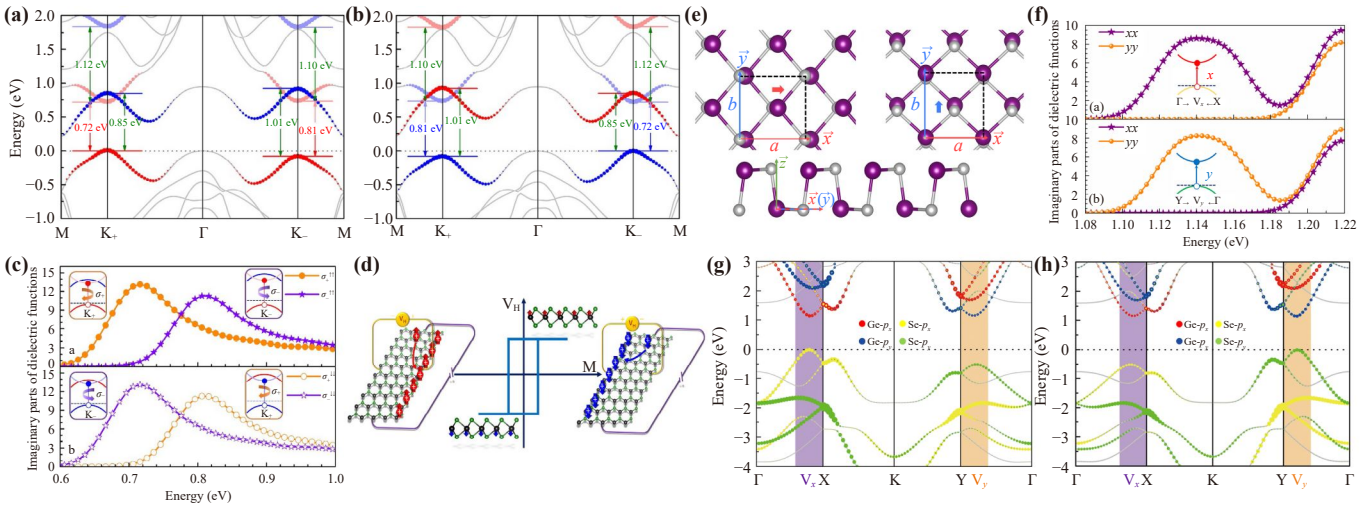

Fig. 1 **(a, b)** Band structures of PV and FV states in 2H-VSe_2 [18]. **(c)** Imaginary parts of complex dielectric function ε_2 for the FV VSe_2 [18]. **(d)** Sketch of data storage utilizing hole-doped FV materials based on AVHE [18]. **(e)** Crystal structures of monolayer GeSe along x-axis and y-axis [26]. **(f)** The ε_2 excited by linearly x-polarized and y-polarized lights and **(g, h)** band structures of GeSe monolayer in P_x and P_y state [26].

strong SOC and opening a new route to overcome the limitations of conventional materials in terms of available systems and tuning flexibility. This review aims to systematically summarize the research progress of AMFV materials, covering their physical mechanisms, modulation methods, and material systems, to provide a comprehensive perspective for researchers in related fields and inspire subsequent exploration and device innovation.

2 Traditional valley-polarized materials

Intrinsic VP is a core focus of FV material research. Its key advantage lies in achieving stable VP without modulation by external fields (magnetic/optical fields) modulation, relying solely on intrinsic spontaneous symmetry breaking of materials (e.g., magnetic order, electric polarization). This characteristic greatly reduces the dependence of traditional valleytronic materials on external stimuli. Based on the physical nature of polarization origins, such materials are currently categorized into three main types: ferromagnetic, ferroelectric, and ferroelastic materials, each of which exhibits unique advantages in mechanism innovation and device applications.

2.1 Ferromagnetic and ferroelectric FV materials

Ferromagnetic FV materials represent a breakthrough in valleytronic research. In conventional transition metal dichalcogenides (TMDs), the VP is largely an external-field-induced and volatile phenomenon [8, 13, 61–64], as the intrinsic SOC alone is insufficient to break the energy degeneracy between K^+ and K^- valleys and induce spontaneous VP. In 2016, theoretical predictions revealed that the intrinsic ferromagnetism of 2H-VSe_2 endows the system with the intrinsic exchange interaction of V-3d electrons, which can spontaneously break time-reversal symmetry [Figs. 1(a, b)]. Combined with the inherent strong SOC of heavy transition metal TMDs that strongly couples the spin and valley degrees of freedom of electrons, this synergetic effect effectively lifts the energy degeneracy between K^+ and K^- valleys and induces stable spontaneous VP at room temperature.

Originating from the SOC-induced spin-valley locking effect, the K^+ and K^- valleys obey strict circularly-dependent optical selection rules, where the K^+ and K^- valleys can only be excited by left-handed σ_+ and right-handed σ_- circularly polarized light, respectively [Fig. 1(c)]. When an external magnetic field switches the magnetization direction of FV materials, both the VP and corresponding optical response reverse simultaneously. In addition, SOC modulates the valley-dependent distribution of Berry curvature in the k-space, and the spontaneous VP further leads to the asymmetric Berry curvature of K^+ and K^- valleys, which is the core physical origin of the anomalous valley Hall effect (AVHE) observed in 2H-VSe_2 and similar FV materials. Based on the AVHE, prototype memory devices with electrical reading and magnetic writing functions can be constructed, realizing nonvolatile valleytronic information storage [Fig. 1(d)] [18].

A remarkable electronic state, known as the half-valley metal, has also been discovered in ferromagnetic FV systems [65–68]. Taking 2H-$FeCl_2$ as an example, by tuning the electron correlation strength, one valley can exhibit metallic behavior while the other remains semi-

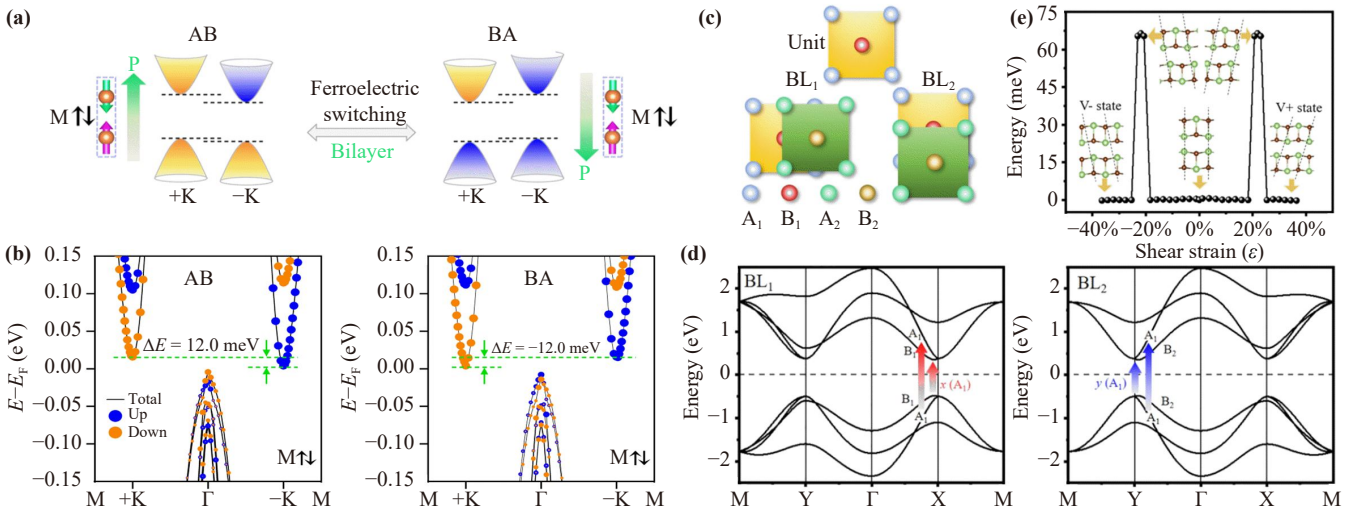

Fig. 2 **(a)** Switching mechanism of VP by interlayer sliding and **(b)** band structures of $VSiGeP_4$ bilayer with AB and BA states [27]. **(c)** Crystal structure of GaBr bilayers. **(d)** Band structures of GaBr bilayer in BL_1 and BL_2 states [36]. **(e)** Energy vs. shear strain under different shear strains for GaBr bilayer [36].

conducting under the combined regulation of SOC and exchange interaction. In such a half-valley metal system, the spin-valley locking effect derived from SOC is still preserved, resulting in selective absorption of a specific helicity of circularly polarized light [65]. Theoretical calculations suggest that topological devices based on half-valley metals could achieve lower energy consumption and higher stability in quantum computing, making the experimental synthesis of related materials a current research focus [69].

Ferroelectric FV materials provide a low-power electrical route for manipulating VP, effectively overcoming the reliance on magnetic fields required in ferromagnetic systems [70–75]. In intrinsic orthorhombic ferroelectric GeSe [26], the inequivalent valleys are located at the X and Y points, enabling coupled FE and FV properties [Fig. 1(e)]. When GeSe transitions from the paraelectric to the ferroelectric phase, the system shifts from a paravalley (PV) to the FV state, inducing pronounced VP [Figs. 1(g, h)]. The valence-band maximum and conduction-band minimum of GeSe are mainly composed of p_x and p_y orbitals, which lead to optical selectivity dependent on x- and y-linearly polarized light [Fig. 1(f)]. In addition, sliding ferroelectric FV systems represent a recently developed class of materials in which interlayer atomic sliding enables switching between different stacking configurations, providing a versatile platform for coupling FE with FV properties [Fig. 2(a)] [20, 36, 37, 76–78]. For instance, when bilayer VS_2 slides from AA to AB stacking, the built-in electric field induced by sliding FE drives band splitting, induces pronounced VP and thereby achieving a three-way coupling among FM, FE, and FV order [78]. Similar behavior has been observed in bilayer $VSiGeP_4$ [Fig. 2(b)], YI_2 and other systems [20, 27, 79–81].

2.2 Other induction mechanisms of FV materials

Moreover, even in stacking structures that retain global inversion symmetry, specific sliding operations can break local symmetry and induce VP [36, 37]. This has led to the proposal of a new VP mechanism that does not rely on breaking either time-reversal or spatial-inversion symmetry, moving beyond the conventional requirement of ferromagnetic or ferroelectric order to lift valley degeneracy. For example, bilayer GaBr in a stable sliding-stacked state can achieve a valley splitting as large as 226.2 meV while preserving global inversion symmetry [Figs. 2(c, d)] [36]. It exhibits FV–FA coupling, enabling VP manipulation via shear strain [Fig. 2(e)]. Similarly, $RhCl_3$ and InI bilayers remove valley degeneracy by breaking the rotational symmetry within individual layers, yielding valley-splitting magnitudes comparable to those in conventional FV materials [37]. All these systems exhibit clear valley-dependent linear-polarization optical selectivity, offering a direct experimental signature for detection. In terms of control, VP in such sliding systems can be efficiently switched via shear strain or interlayer sliding, overcoming the limitations of electric-field manipulation in inversion-symmetric structures [Fig. 2(e)].

2.3 Properties and application prospects of VP materials

Valleytronics transcends the dependence of traditional electronics on charge and spin. By regulating valley states through various means such as light, electricity, magnetism, stress, and non-Hermitian physics, it demonstrates broad application potential in fields such as information storage, logic operations, quantum technolo-

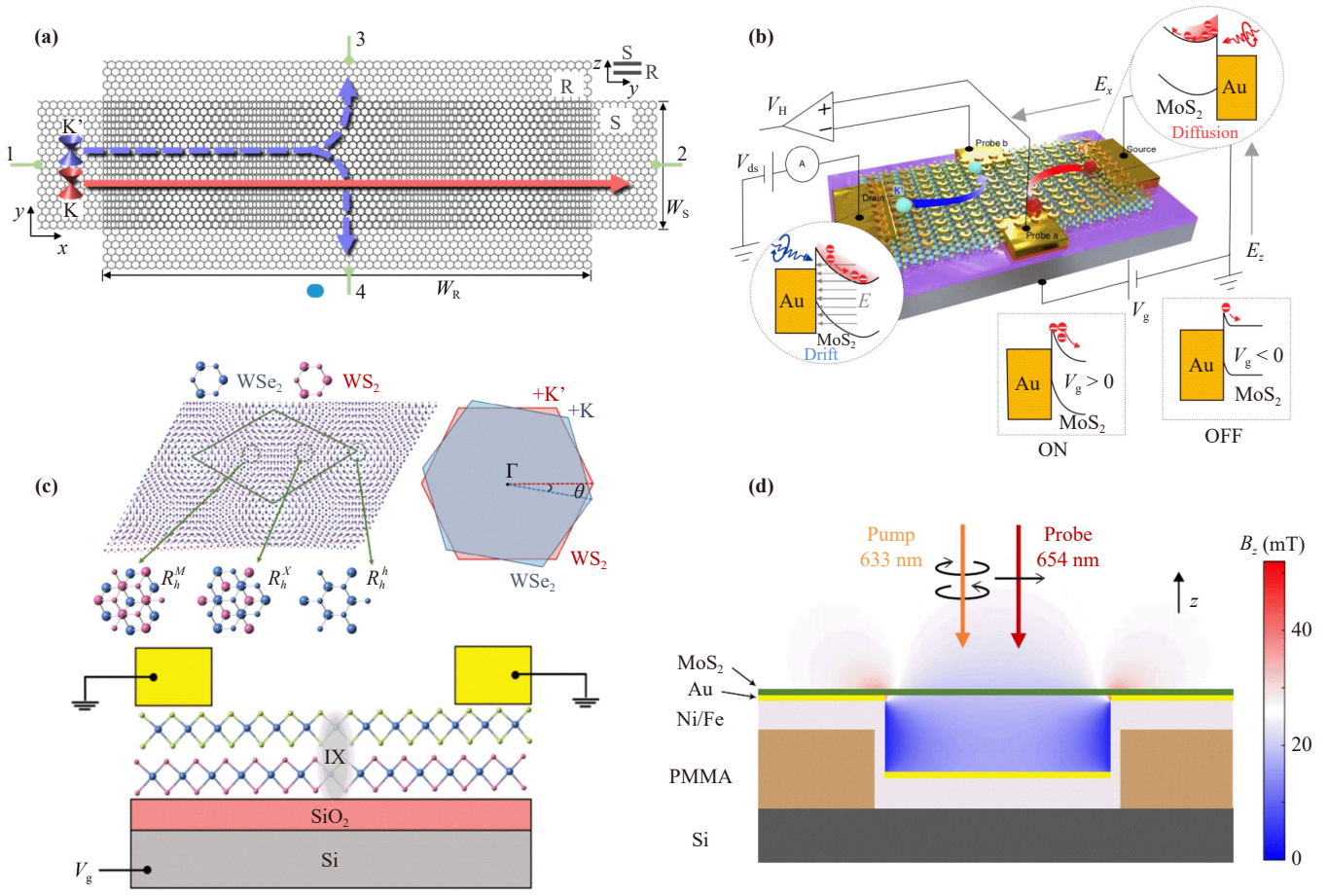

Fig. 3 **(a)** Schematic of the non-Hermitian moiré valley filter based on graphene layers [83]. **(b)** Device configuration and experimental set-up for MoS_2 valleytronic transistor [84]. **(c)** Moiré pattern formed by stacking two WSe_2/WS_2 bilayers, its Brillouin zone with a twist angle of θ, and device schematic [86]. **(d)** Cross-sectional schematic of valley-mechanical device, which consists of a monolayer MoS_2 suspended over square hole structures conformally coated with Ni/Fe permalloy films [2].

gies, photoelectric conversion, and sensing [2, 6, 9, 82]. Currently, valleytronics has gradually progressed from fundamental research toward device implementation and functionalization, relying on properties such as symmetry breaking in two-dimensional materials, valley-spin coupling, and valley-selective optical selection rules. For instance, a non-Hermitian valley filter based on bilayer graphene moiré superlattices can achieve nearly 100% VP efficiency, and its gate-tunable characteristics offer a new approach for high-precision valley electron sources [Fig. 3(a)] [83]. As a core device, valley transistors have also developed various high-performance configurations [Fig. 3(b)]: the room-temperature type achieves valley-polarized injection and electrical detection via plasmonic antennas, with an on-off ratio of up to 10^3 [84]; the piezoelectric type utilizes strain-induced piezoelectric fields to significantly enhance the operational frequency of valley quantum bits [85]. In optoelectronic devices and non-volatile memory, by tuning the twist angle of WSe_2/WS_2 heterostructures, electrically controlled VP switching and photon spin encoding can be realized, laying the foundation for the development of electrically controlled valley-spin memory [Fig. 3(c)] [86]. Additionally, valley information can couple with mechanical motion, enabling the transduction of valley states into mechanical displacement using a monolayer MoS_2 resonator [Fig. 3(d)] [2]. Moreover, the valley degree of freedom provides new insights for quantum computing encoding and topological state regulation. Through mechanisms such as valley-spin locking and the valley Zeeman effect, efficient manipulation and readout of quantum states are achieved [87–90]. Valleytronics is expected to overcome the power consumption and integration bottlenecks of traditional electronics, offering a novel solution for the next generation of highly efficient and low-power electronic technologies.

As listed in Table 1, the FV materials rely on strong SOC or symmetry breaking to achieve VP, which not only restricts material selection but also makes efficient electrical control challenging. Therefore, exploring new VP mechanisms that do not depend on strong SOC and are compatible with efficient electrical control is of

Table 1 Comparison between ferromagnetism (FM), antiferromagnetism (AFM), altermagnetism (AM), ferrovalley (FV), and altermagnetic ferrovalley (AMFV).

Property	FM	AFM	AM	FV	AMFV
Spin alignment	Parallel spin	Antiparallel spin	Antiparallel spins	Parallel spin	Antiparallel spins & SVL
Net magnetization	Non-zero	Zero	Zero	Non-zero	Zero
Spin splitting	Present due to spin alignment	Absent or negligible	Present due to symmetry-induced effects (SOC-free)	Present (strong SOC-dependent)	Present (non-relativistic symmetry + valley splitting)
Time-reversal symmetry	Broken	Preserved	Broken	Broken (spontaneous VP)	Broken
Spin–orbit coupling (SOC)	Often significant	Negligible	Not required for spin splitting	Indispensable	Not required for spin-valley locking
Anomalous Hall effect (AHE)	Present	Absent	Present (zero net magnetization)	AVHE	Both AHE & AVHE
Spin/valley transport	Strong spin polarization with stray fields	Weak/absent spin polarization, no stray fields	Strong spin polarization, no stray fields	Valley-polarized transport, spin-valley coupling	Spin-valley-optical locked transport
Core freedom	Spin	Spin	Momentum-dependent spin	Electron valley (K^+/K^-)	Spin, valley, optical, layer
Typical materials	Fe, Ni, Co	MnO, NiO	RuO_2, MnTe, Mn_5Si_3, CrSb	Monolayer VSe_2, GeSe	V_2Se_2O, Fe_2MX_4, $Ca(CoN)_2$

great importance. In recent years, the emergence of altermagnetism, with its unique momentum-space spin splitting characteristics, offers a promising solution and has given rise to the new research direction of AMFV materials.

3 Altermagnetic materials

3.1 Overview of altermagnetism

Altermagnetism [see Fig. 4(a)] is an emergent class of magnetic materials that revolutionizes the traditional magnetic classification system. Its defining characteristic is non-relativistic spin splitting in reciprocal space, a unique property that opens new avenues for magnetic manipulation [38, 39, 42, 50, 91–101]. Compared to conventional magnetic materials, altermagnets possess a compensated magnetic order with zero net magnetic moment in real space, inheriting the stray field-free stability of antiferromagnets. Meanwhile, they show significant spin polarization (SP) in reciprocal space, retaining the readily tunable magnetoelectric response of ferromagnets. Based on differences in magnetic moment arrangement and coupling with electronic band characteristics, altermagnets can be classified into various types such as *d*-wave, *g*-wave, and *i*-wave [38, 39]. Each category shows distinct differences in spin splitting symmetry and charge transport efficiency, providing diverse options for targeted applications. Recently, the experimental confirmation of altermagnetism has been firmly established through the direct detection of momentum-space spin splitting via spin-resolved angle-resolved photoemission spectroscopy (ARPES) in bulk single crystals such as CrSb, RuO_2 and MnTe [48, 49, 102–108]. To date, the development of altermagnets has been particularly rapid, gradually giving rise to other types of altermagnetism, such as spin-cluster altermagnetism [109], spin-orbital altermagnetism [110], orbital altermagnetism [111], and charge-order-induced altermagnetism [112]. Application bottleneck of altermagnetism lies in achieving efficient and non-volatile external regulation of spin splitting. Current research mainly pursues breakthroughs through two pathways. The first is coupling AM with other ferroic orders such as FE and FA to construct multiferroic systems, and precisely regulating its spin properties via ferroic order switching (e.g., ferroelectric polarization switching and ferroelastic lattice rotation). The second is utilizing twist engineering to break the system symmetry of 2D bilayers, thereby inducing stable altermagnetism.

3.2 Altermagnetism and multiferroic coupling

From the perspective of the multiferroic coupling, different types of ferroic orders achieve flexible regulation of altermagnetism through unique pathways [113–121]. Among them, the coupling between FE and altermagnetism is the synergistic regulation of electron spin and magnons via polarization switching [Fig. 4(b)] [113]. For example, in monolayer $CrPS_3$, when the ferroelectric polarization is reversed from the P state to the $-P$ state, the sign of spin splitting is simultaneously reversed with a switching barrier of only 0.17 eV/u.c. [116]. Systems such as wurtzite w-MnSe exhibit excellent room-temperature application potential, with a large ferroelectric polarization of 53 $\mu C/cm^2$ and a significant spin splitting

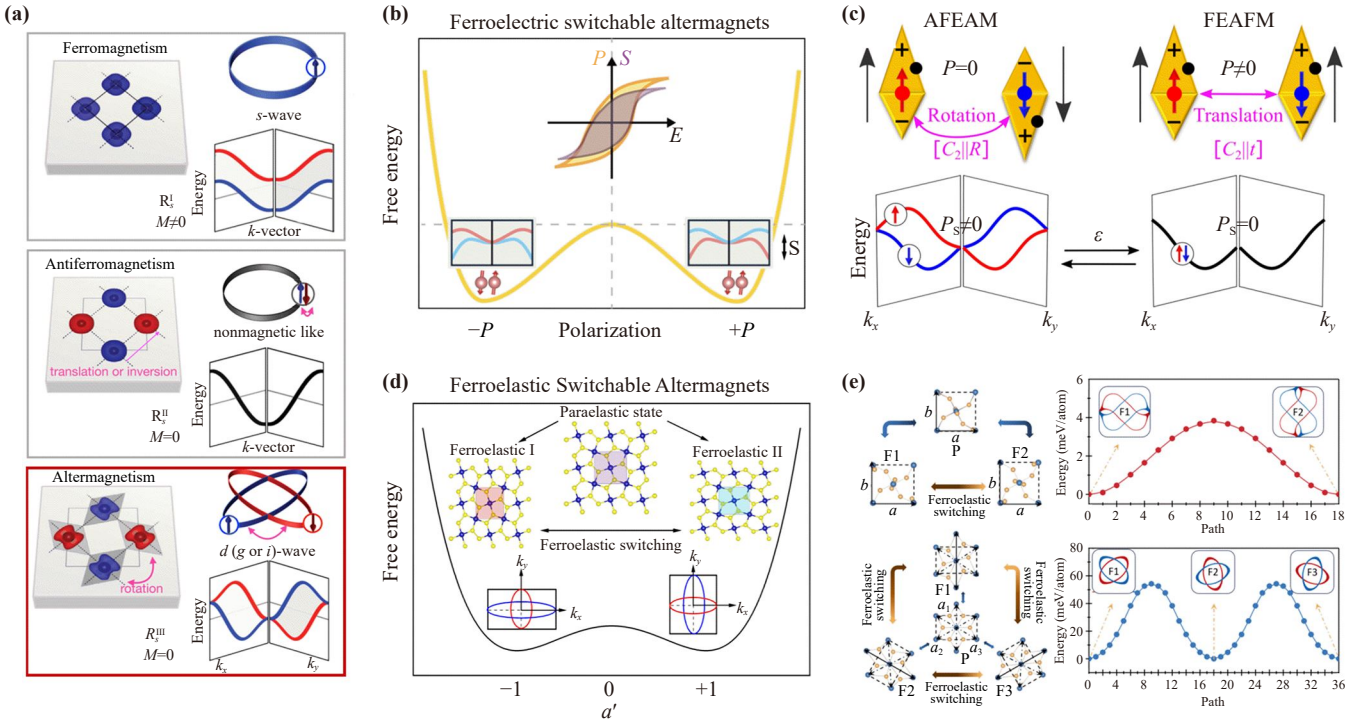

Fig. 4 **(a)** Illustrative models of collinear ferromagnetism, antiferromagnetism, and altermagnetism in crystal-structure real space and nonrelativistic electronic-structure momentum space [39]. **(b)** Schematic illustration of ferroelectric switchable altermagnetism [113]. **(c)** The design principle for AFEAM and FEAFM [114]. **(d)** Schematic illustration of ferroelastic altermagnetism and its switching [124]. **(e)** Schematic diagram of 2-state and 3-state ferroelastic switching and energy profiles in RuF_4 and CuF_2 monolayers [115].

of 245 meV [122]. In addition, altermagnetism can couple with antiferroelectricity (AFE) [Fig. 4(c)], giving rise to the antiferroelectric altermagnets (AFEAM) [114]. For example, in the AFE state of $CuWP_2S_6$, the spin splitting reaches 120 meV. When the system transforms to the FE state via a weak electric field, the spin splitting effect vanishing. Similarly, the G-type antiferromagnetic $BiCrO_3$ with AFE state is a typical AFMAM candidate, which transforms into an AFM in the FE phase [114]. Additionally, FA mainly dominates the regulation of altermagnetism through lattice distortion or lattice rotation [123]. For example, ferroelastic switching in pentagonal monolayer $CoSe_2$ not only drives a 90° rotation of the spin-split bands but also regulates the sign of the magneto-optical Kerr effect through the co-directional/counter-directional rotation of the lattice and Néel vector [Fig. 4(d)] [124]. Monolayers RuF_4 or CuF_2 can achieve two-state or three-state spin splitting switching via $\pi/2$ or $2\pi/3$ lattice rotation with low switching barriers, showing promise for efficient encoding of multi-state spin information [Fig. 4(e)] [115]. A hydroxylated monolayer $Mn_2B_2(OH)_2$ further realizes the synergy between chemical and ferroelastic regulation, yielding a spin splitting as high as 1130 meV, while enabling simultaneous control of altermagnetism [123].

3.3 Twist-induced altermagnetism

Beyond the ferroic order coupling, twist technology provides a universal and efficient strategy for constructing altermagnets in 2D systems [125–128]. A 2023 study pioneered the core idea of inducing spin splitting via twisted interlayer AFM bilayers. Twisting can break spin degeneracy symmetry, inducing momentum-dependent non-relativistic spin splitting in the absence of SOC, with an effect comparable to SOC in heavy elements. This phenomenon has been verified in 2D materials like $NiCl_2$, CrI_3, CrN, and CrSBr [Fig. 5(b)], laying the experimental foundation [125]. A 2024 study further established a universal framework defining the three-step standardized process of stacking-flipping-twisting [Fig. 5(a)]. Stacking monolayers to form an interlayer AFM bilayer, then flipping the upper layer to introduce in-plane twofold rotational symmetry, and reversing the twist to break inversion symmetry, ultimately inducing stable AMs [126]. Compatible with all 2D Bravais lattices, this framework enables customization of various waveforms (e.g., *d*-wave, *g*-wave and *i*-wave), and can optimize performance by adjusting twist angle and Fermi level. These strategies enrich the regulatory dimensions of altermagnetism and promote its applications

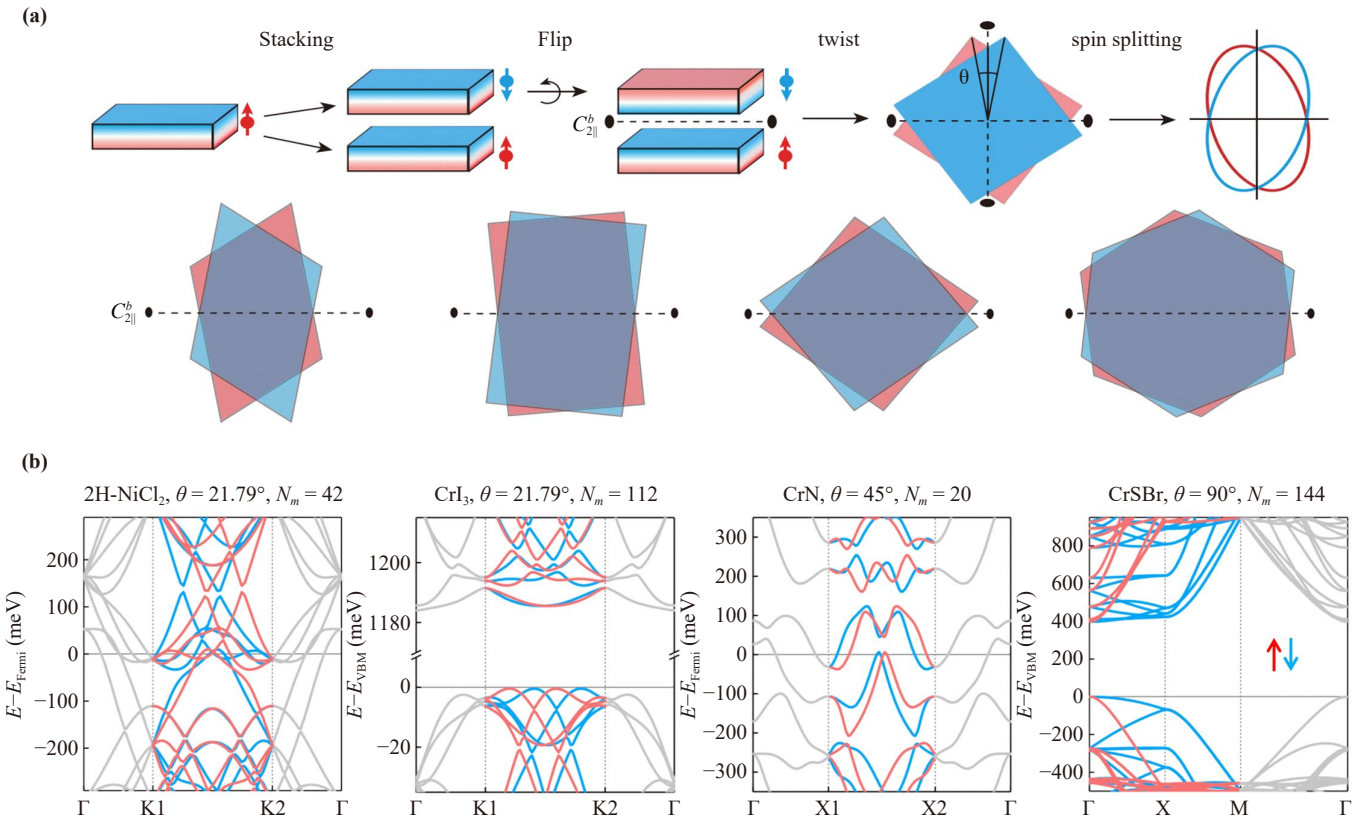

Fig. 5 **(a)** Illustration of a general route to altermagnetism in twisted magnetic Van der Waals (MvdW) materials and its corresponding key C_{2k} symmetry (dashed lines) in twisted bilayers of any 2D MvdW material with one of the five 2D Bravais lattices, inducing altermagnetism [126]. **(b)** Band structures of twisted 2H-phase $NiCl_2$, hexagonal CrI_3, CrN and rectangular CrSBr bilayers [125].

4 Altermagnetic ferrovalley materials

AMFV materials integrate altermagnetism with FV properties, enabling spontaneous VP within altermagnet systems [57, 60, 129–131]. Such non-relativistic valley polarization, independent of SOC, arises from broken PT symmetry in altermagnetic lattices, following the crystal symmetry-paired (C-paired) mechanism rather than the conventional SOC-dependent time-reversal symmetry-paired (T-paired) mechanism, and is supported by a minimal tight-binding model in many previous studies [57, 60, 132]. Their defining feature is the locked relationship between spin and valley degrees of freedom, which can be controlled through strain, stacking, sliding, twisting and proximity effects to create stable VP state in momentum space. Furthermore, the valley-dependent optical selection rules of polarized light in valleys provides a novel physical mechanism for information encoding and photoelectric detection. The coupling of spin, valley, optics, and layer degrees of freedom opens new directions for designing functional devices and shows broad application prospects in non-volatile memory and quantum information processing.

In AMFV systems, spin-group symmetries produce valley-dependent Berry curvature with an anisotropic distribution, which directly leads to the anomalous valley Hall effect. These systems also host rich topological band crossings, such as spin-resolved Weyl points and symmetry-protected second-order topological corner states. Fundamentally, altermagnetism-driven spin–valley locking unifies the crystal valley Hall effect, quantum anomalous Hall effect, and spin-resolved topological corner states into a complete topological-valley-spin framework [60, 101, 133–135]. The core modulation mechanisms of VP in AMFV materials are detailed in the following sections, along with a brief analysis of their relative strengths and limitations, thereby providing valuable references for the rational design of related device.

4.1 Strain manipulation of VP in AMFV

In 2021, the phenomenon of C-paired spin-valley locking (SVL) mediated by crystal symmetry was first revealed in V_2Se_2O [Figs. 6(a, b)] [57]. Unlike traditional transition metal dichalcogenides (TMDs), which rely on strong SOC and T-paired mechanisms, the spin splitting in V_2Se_2O-like materials originates from the strong

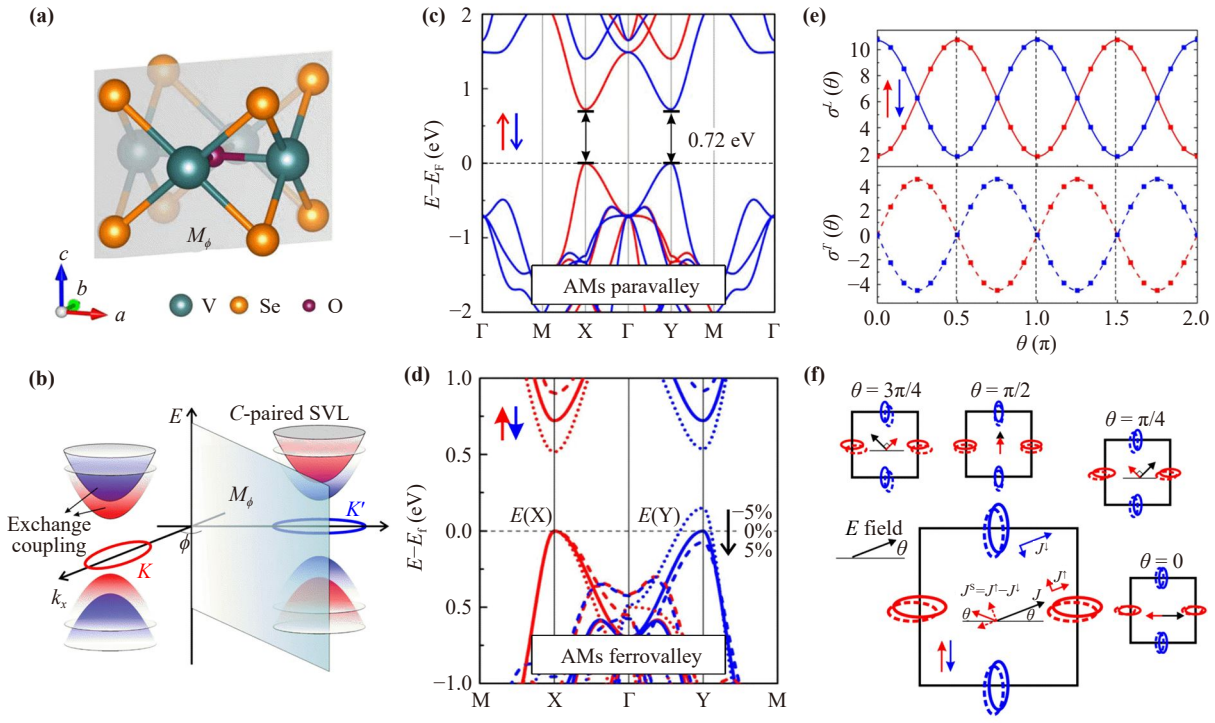

Fig. 6 **(a)** Crystal structure of V_2Se_2O monolayer [57]. **(b)** C-paired SVL and spin splitting protected by the mirror M_ϕ crystal symmetry. **(c, d)** Spin-polarized band structures of V_2Se_2O without and with external uniaxial strain. **(e)** Angle-dependence of the longitudinal and transverse charge conductivity varying with the electric field direction. **(f)** Relation between directions of charge current J and spin current J_S.

exchange coupling between itinerant electrons and local magnetic moments of the antiferromagnetic order [58, 134, 136–139]. As shown in Figs. 6(c) and (d), the VP can be induced by breaking symmetry via uniaxial strain alone [140–142]. Under moderate electrostatic doping, it can also exhibit a giant piezomagnetic effect and generate large noncollinear spin currents [Figs. 6(e, f)]. Moreover, constructing a Janus-structured V_2SeTeO/V_2STeO monolayer not only retains the in-plane C-paired spin-valley locking, but also breaks the out-of-plane mirror symmetry, resulting in giant piezoelectric properties [58, 143]. This creates a multiply coupled system allowing independent tuning of piezoelectric, piezovalley, and piezomagnetic responses [58, 143, 144]. In addition, research on higher-order topological physics has further expanded the physical implications of AMFV materials, extending investigations from spin-valley manipulation to the field of corner electronics [133, 145, 146]. Related studies, based on effective models, have established a spin-corner locking mechanism and realized a spin-resolved second-order topological insulating state in two-dimensional AMFV systems such as CrO and Cr_2Se_2O.

4.2 Electric field tuning of VP in AMFV

The $A(BN)_2$-type materials represented by $Ca(CoN)_2$ are typical AMFV systems with layer-resolved spin-valley locking characteristics [59, 147]. Their core advantage lies in the efficient electric field modulation of VP via gate voltage, which simultaneously manipulates the spin polarization state [Figs. 7(a–c)]. By substituting the top-layer Co atoms in $Ca(CoN)_2$ with Fe to form the Janus $CaCoFeN_2$ structure [Fig. 7(d)], an orthorhombic ferrimagnetic ground state is obtained. This structure exhibits giant spontaneous valley splitting in the absence of SOC [Fig. 7(e)] [148]. This behavior originates from a triple mechanism: symmetry breaking, enhanced valley-layer locking driven by an internal electric field, and ferrimagnet-mediated spin-valley locking. The valley splitting strength can be flexibly tuned via uniaxial strain and external electric fields. Moreover, the material shows highly anisotropic spin-plasmon characteristics, with direction-dependent responses to both static electric fields and dynamic electromagnetic waves. Strain can reverse the VP direction [149, 150]. Studies on such layer-resolved AMFV materials have elucidated the core mechanism of layer-resolved spin-valley locking. Through multi-dimensional control strategies — such as electric fields and strain — along with device design, these materials provide a representative example for the practical application of AMFV systems in spintronics and valleytronics.

4.3 Interlayer sliding modulating of VP in AMFV

Sliding, as an effective means of inducing altermag-

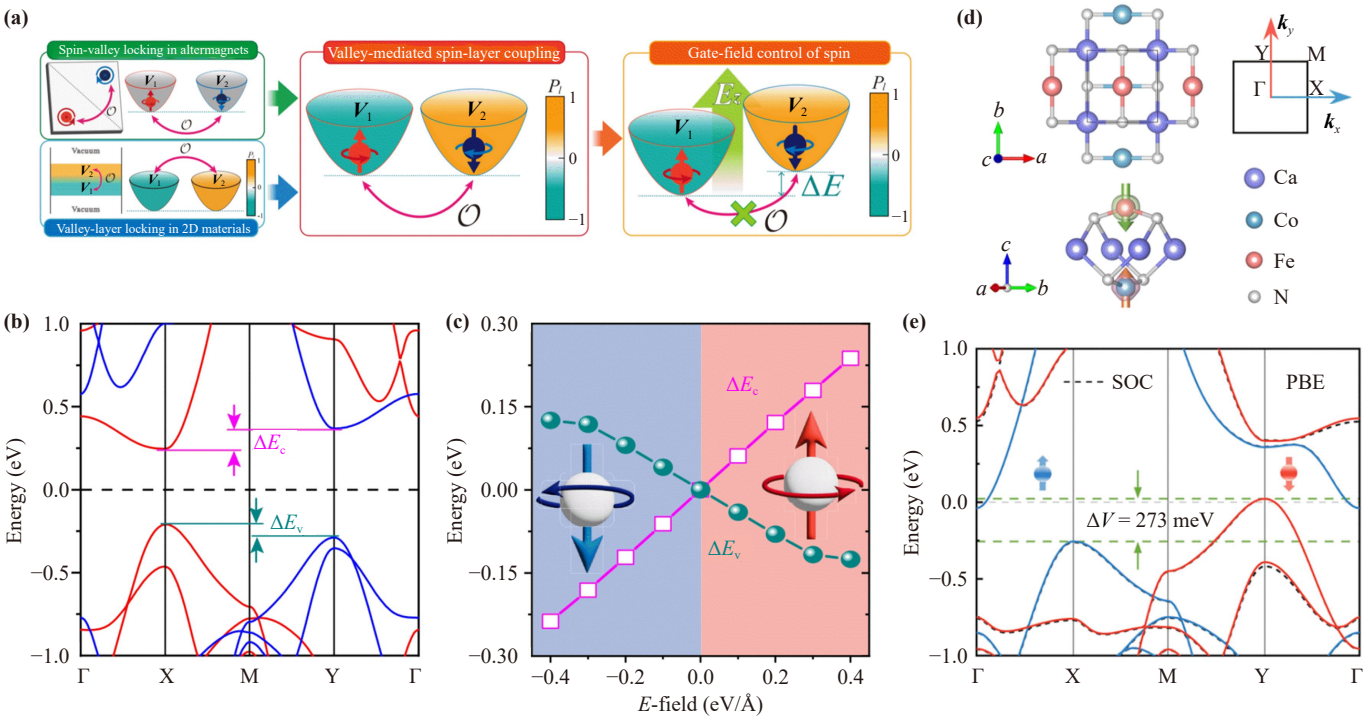

Fig. 7 **(a)** Illustration of the mechanism of valley-mediated spin-layer coupling and the gate-field control of spin. **(b)** Band structure of $Ca(CoN)_2$ under a gate field of $E_z = 0.2$ eV/Å. **(c)** Valley splitting for VBM (ΔE_v) and CBM (ΔE_c) versus E_z of $Ca(CoN)_2$ [59]. **(d, e)** Geometric structure and electronic band structures of Janus $CaCoFeN_2$ monolayer [148].

netism, also serves as one of the effective approaches for regulating AMFV state [132, 151–154]. The Fe_2MX_4 (M = W, Mo, etc.; X = S, Se, Te, etc.) family [Fig. 8(a)] has been identified as a new class of 2D tetragonal AMFV materials with room-temperature application potential [60]. In the absence of SOC, Fe_2MX_4 exhibit zero Berry curvature everywhere in the Brillouin zone. When SOC is included, M_{xy} mirror and $S_{4z}T$ magnetic group symmetries ensure opposite Berry curvatures at the high-symmetry X and Y points, which forms the core origin of the crystal valley Hall effect. Under biaxial compressive stress, Fe_2MX_4 materials transform from the altermagnetic semiconductor phase into a bipolarized topological Weyl semimetal phase, exhibiting symmetry-protected Weyl points.

A key breakthrough of these *d*-wave altermagnets lies in the first identification of an observable physical quantity directly linked to the FV state: linearly optical dichroism [Fig. 8(b)]. In these systems, the spin-up X valley absorbs the *y*-polarized light (σ_y), while the spin-down Y valley absorbs only *x*-polarized light (σ_x) [Fig. 8(d)], forming a robust spin-valley-optical triple locking that is independent of SOC. This discovery provides a direct optical signal for non-contact and non-destructive detection of the FV state in AMFV materials, with distinct characteristics and practical implications compared to conventional optical probes: unlike circular dichroism in traditional SOC-based valleytronic materials (e.g., monolayer MoS_2, WSe_2 [10, 85]. The sensitivity of linear optical dichroism for AMFV detection is primarily constrained by valley splitting magnitude (reliably detectable above ~100 meV, e.g., 0.29 eV in Fe_2WTe_4 bilayers [132], while signals below 50 meV are easily masked by noise) and sample quality. Importantly, linear optical dichroism is well-suited for room-temperature detection due to that the altermagnetic order in Fe_2MX_4 (e.g., Fe_2WSe_4) remains stable up to 330 K.

In bilayer systems, sliding enables the transition from a PV state (AB stacking) to non-volatile FV states (AC_1/AC_2 stacking), inducing a giant VP of up to 0.29 eV and optical dichroism [Fig. 8(c)], which in turn triggers unequal absolute values of the Berry curvature leading to the AVHE [Fig. 8(e)] [132]. By adjusting the doping type, opposite transverse Hall voltages can be observed, offering a clear implementation pathway for designing non-volatile memory devices based on the mechanical sliding-based writing and electrical signal reading principle.

Furthermore, changing the magnetization direction constitutes another crucial dimension for inducing and switching the valley-polarized state in the presence of SOC. When the magnetic moment is oriented out-of-plane (along the *z*-axis) or at a 45° direction, the $Fe_2MoS_2Se_2$ system retains $C_{4z}T$ magnetic group symmetry, leaving the X and Y valleys equivalent and non-polarized (PV state). However, when the magnetic moment rotates to an in-plane direction (*x* or *y* axis), it breaks the C_{4z} lattice rotational symmetry, inducing a

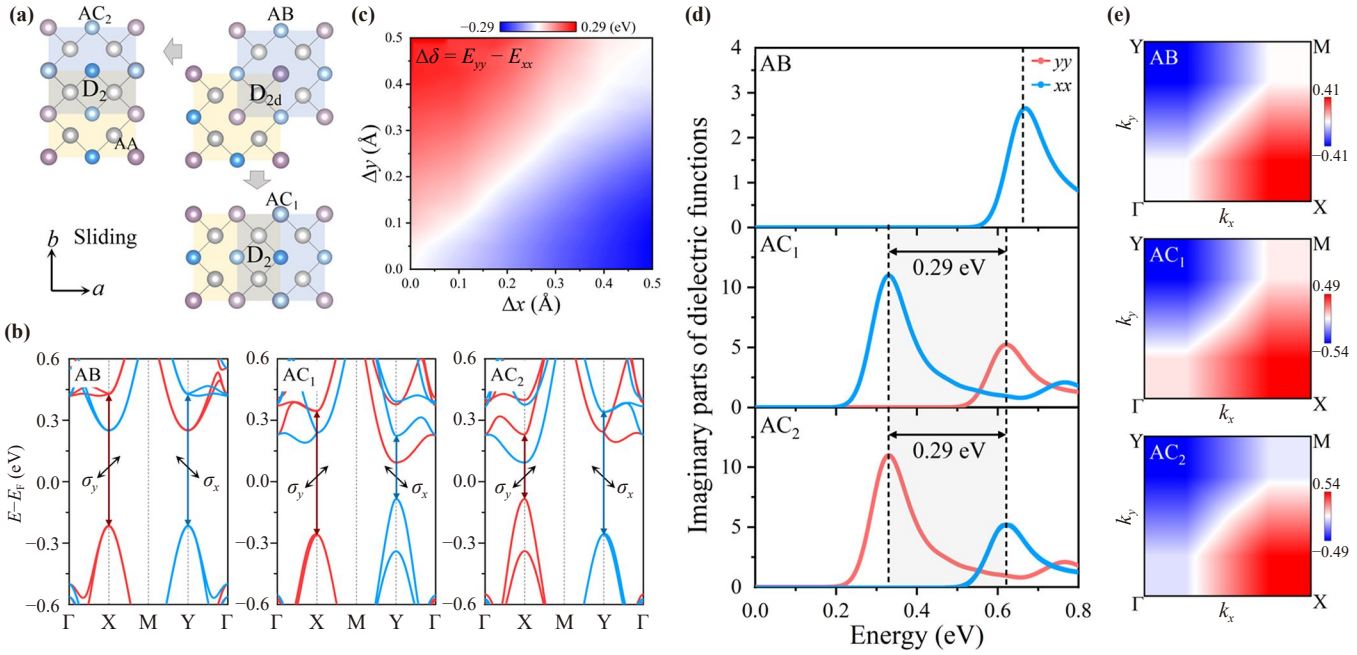

Fig. 8 **(a)** Schematic structure of the Fe_2MX_4 bilayers [132]. **(b)** VP difference contour versus (Δx, Δy) of Fe_2WTe_4 bilayer. **(c)** Spin-projected band structures without SOC of AB, AC_1 and AC_2 states. **(d)** Imaginary parts of complex dielectric function ε_2 and **(e)** contour maps of Berry curvatures in units of Å^2 in 2D Brillouin zone in Fe_2WTe_4 bilayers.

VP of 1.6 meV (FV state), which can be further enhanced by heavy-element doping to strengthen SOC [155]. This mechanism provides another universal strategy for regulating FV states, further expanding the application prospects of such materials in multifunctional valleytronic devices.

4.4 Twisting modulating of VP in AMFV

In traditional 2D materials, twisting is often employed as an efficient way to manipulate degrees of freedom [86, 156, 157]. For AMFV materials, twisting can induce magnetic phase transition by modulating lattice symmetry and interlayer interactions, and when combined with an out-of-plane electric field, it enables flexible control of VP [Fig. 9(a)] [156]. Research in 2023 confirmed that twisting can break the fourfold spin degeneracy symmetry in two-dimensional antiferromagnetic materials [125]; the establishment of a standardized stacking-flipping-twisting framework for valley-related engineering in 2024 further demonstrated that this strategy is applicable to all two-dimensional Bravais lattices, laying the groundwork for developing valley-related functionalities [126]. In an AMFV bilayer formed via twisting, there exist degenerate valleys originating from different layers with opposite SP. Applying an out-of-plane electric field creates a layer-dependent electrostatic potential, causing the energy levels of these valleys to stagger and lift their degeneracy, thereby generating VP, and reversing the electric field direction allows for opposite control of VP. For instance, in bilayer VOBr with a twist angle of 48.16°, applying an out-of-plane electric field of 0.02 V/Å leads to pronounced valley splitting in the conduction band, successfully achieving SP and VP [Fig. 9(c)] [156]. Meanwhile, monolayer $Ca(CoN)_2$ [Fig. 9(b)], as a special altermagnet, exhibits valley splitting of 125 meV in the conduction band and 21 meV in the valence band under a 0.04 V/Å electric field, further confirming the universality of this approach [Fig. 9(d)] [156]. More importantly, beyond realizing VP, electric-field regulation can also induce key electronic states such as half-spin/valley metals. These states are ideal candidates for building high-performance integrated spintronic-valleytronic devices.

4.5 Proximity effect modulating of VP in AMFV

The altermagnetic proximity effect (AMPE) has emerged as a key method for regulating VP in AMFV materials [158]. Its core mechanism lies in utilizing the van der Waals interface coupling to efficiently transfer the spin texture from an altermagnet to an adjacent non-magnetic layer, thereby breaking valley degeneracy without external fields and enabling efficient VP control [Fig. 10(a)]. For instance, the altermagnetism of V_2Se_2O can transfer its non-relativistic spin texture across the interface to adjacent non-magnetic (NM) layers such as β-SnO, PbS, and PbO, converting them into proximity-induced altermagnets. This process breaks the original spin-valley degeneracy in the non-magnetic layer, with

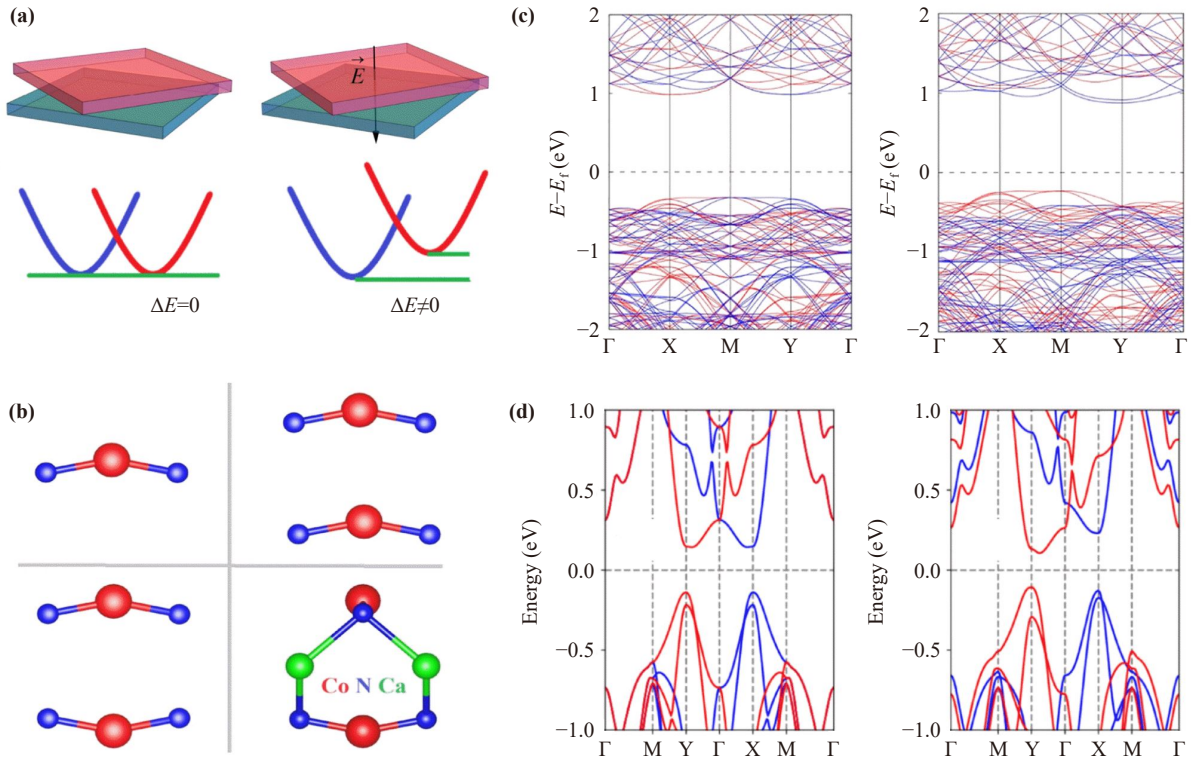

Fig. 9 **(a)** Twisted altermagnetic bilayer without and with an out-of-plane electric field E, and valleys changes near the Fermi level [156]. **(b)** Crystal structure of $Ca(CoN)_2$ monolayer. **(c)** Band structure of VOBr bilayer with the twist angle of 48.16° under $E = 0$ and 0.02 V/Å. **(d)** Band structures of $Ca(CoN)_2$ with $E = 0$ and 0.04 V/Å.

the valley splitting strength decaying monotonically with increasing interlayer distance [159]. The broken mirror symmetry of V atoms in the V_2Se_2O/β-SnO [Fig. 10(b)] induces a net magnetic moment, resulting in VP up to 100 meV. Furthermore, reducing the interlayer distance enhances the net magnetic moment of V atoms induced by AMPE, leading to a significant increase in VP. For example, in V_2Se_2O/β-SnO, reducing the interlayer distance by 0.5 Å can boost the VP to nearly 400 meV [Figs. 10(c, d)]. Additionally, uniaxial strain can further synergistically break the valley degeneracy, enabling fine-tuning of VP. In PbS/V_2Se_2O, applying 3% tensile strain along the x-axis produces a valence band valley splitting of 152 meV. Compared to chemical doping strategies such as substituting V atoms with Cr to form a ferrimagnetic monolayer, the AMPE approach avoids potential structural stability issues and offers greater tunability, providing crucial theoretical support for developing low-power consumption valleytronic devices.

Strain, electric field tuning, interlayer sliding, twisting engineering, and proximity effect represent the main strategies for regulating VP in AMFV materials. These tuning methods, together with their representative materials, achievable VP magnitudes, stability, and inherent pros and cons are systematically summarized and compared in Table 2. Strain engineering can generate large VP with good mechanical stability and compatibility with micro-nano fabrication, but suffers from low dynamic tunability and may cause lattice distortion or phase transition under excessive strain. Electric field modulation enables fast, reversible, low-power VP tuning compatible with semiconductor devices, but requires high-quality dielectrics and may be weakened by built-in electric fields. Interlayer sliding realizes non-volatile VP switching and multistable states for memory applications, but shows low speed, hysteresis, poor repeatability and difficulty in large-scale fabrication. Twisting engineering provides high flexibility and synergistic modulation with electric fields, but demands precise angle control, has low structural stability and produces small VP alone. The altermagnetic proximity effect achieves nondestructive and increases the complexity of device design. Notably, the synergistic combination of multiple tuning strategies can further break valley degeneracy and optimize VP performance, making it more suitable for practical device applications.

5 Potential applications and device concepts of AMFV materials

The unique synergy between FV physics and altermag-

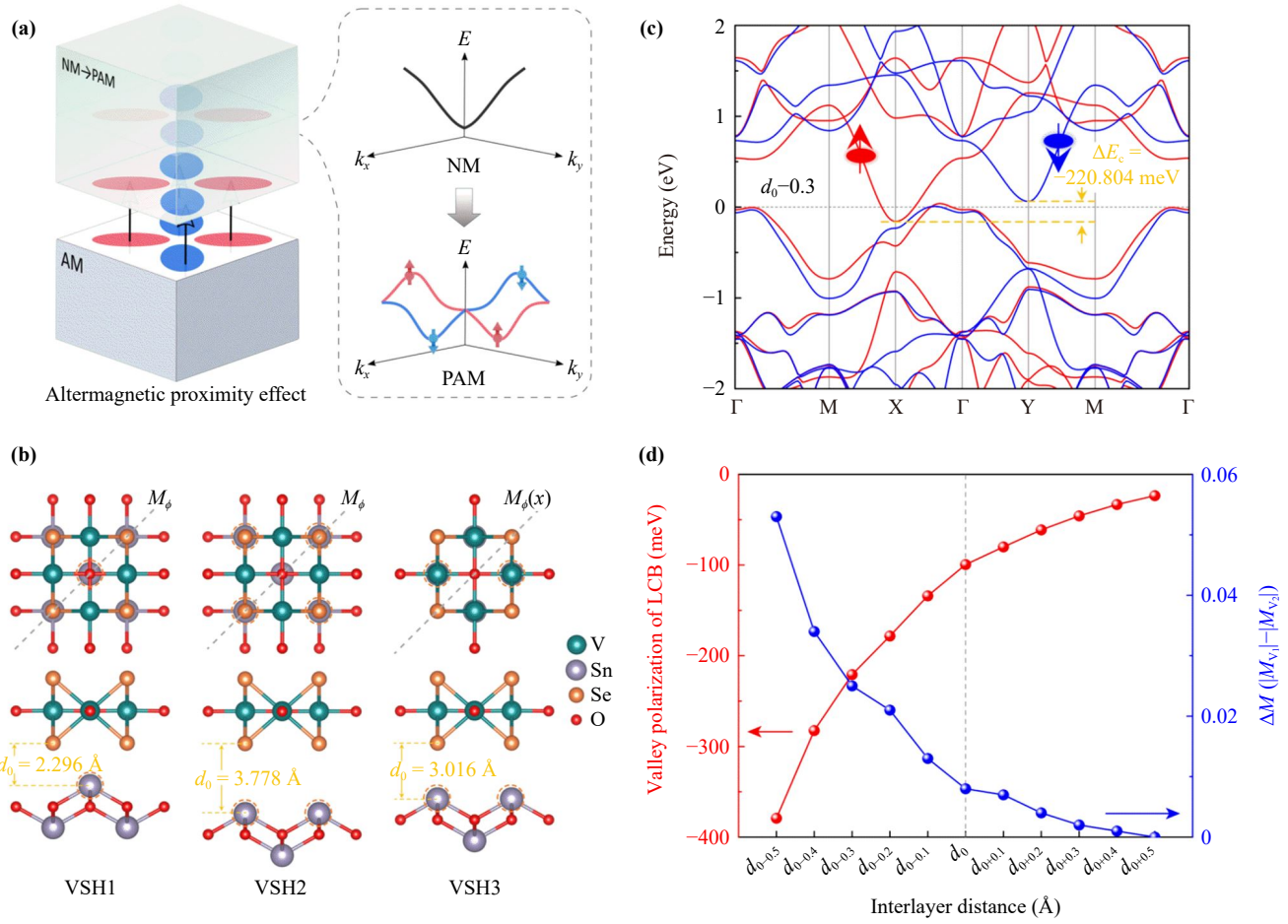

Fig. 10 **(a)** AM order penetrating an NM layer and band evolution of the NM layer as it becomes a proximitized altermagnet [158]. **(b)** Crystal structures of V_2Se_2O/SnO bilayer with different stacking states. **(c)** Spin-polarized band structure of V_2Se_2O/SnO when the interlayer distance is compressed by 0.3 Å. **(d)** Variation of VP with interlayer distance between V_2Se_2O and SnO [159].

netism in AMFV materials provides a novel material foundation for valleytronic devices [59, 144, 160–162]. This fundamentally reduces the reliance on external fields and specific materials, driving innovation in device principles. In terms of device applications, such materials exhibit diverse and efficient design pathways with experimentally achievable high-performance metrics, far exceeding the performance of conventional valleytronic and spintronic devices. Monolayer $Ca(CoN)_2$, utilizing its valley-spin-layer coupling effect, enables the construction of a tunnel junction controllable only by gate voltage, inducing an ultrahigh effective magnetic

Table 2 Summary of valley polarization tuning methods in typical AMFV materials in this work.

Tuning method	Representative material	Maximum VP	Critical tuning condition	Stability/Temperature	Core advantage	Core limitation
Strain engineering	Monolayer V_2Se_2O	~0.72 eV	Uniaxial strain (symmetry breaking)	Room-temperature stable	Giant VP, mechanical compatibility	Low dynamic tunability
Electric field gating	Monolayer $Ca(CoN)_2$	~0.273 eV (valence band)	Out-of-plane E-field	>300 K	Fast, low-power, CMOS-compatible	Requires high-quality dielectrics
Interlayer sliding	Bilayer Fe_2WTe_4	~0.29 eV	AB ↔ AC_1/AC_2 stacking	> 330 K	Non-volatile switching, linear optical dichroism	Slow speed, scaling difficulty
Twist engineering	Twisted bilayer VOBr	Obvious valley splitting	Twist angle	Layer-sensitive	High symmetry tunability	Precise angle control needed
Proximity effect	V_2Se_2O/β-SnO heterostructure	Up to ~0.40 eV	Interlayer distance	Interface-dependent	Non-destructive, giant VP	Defect-sensitive interface

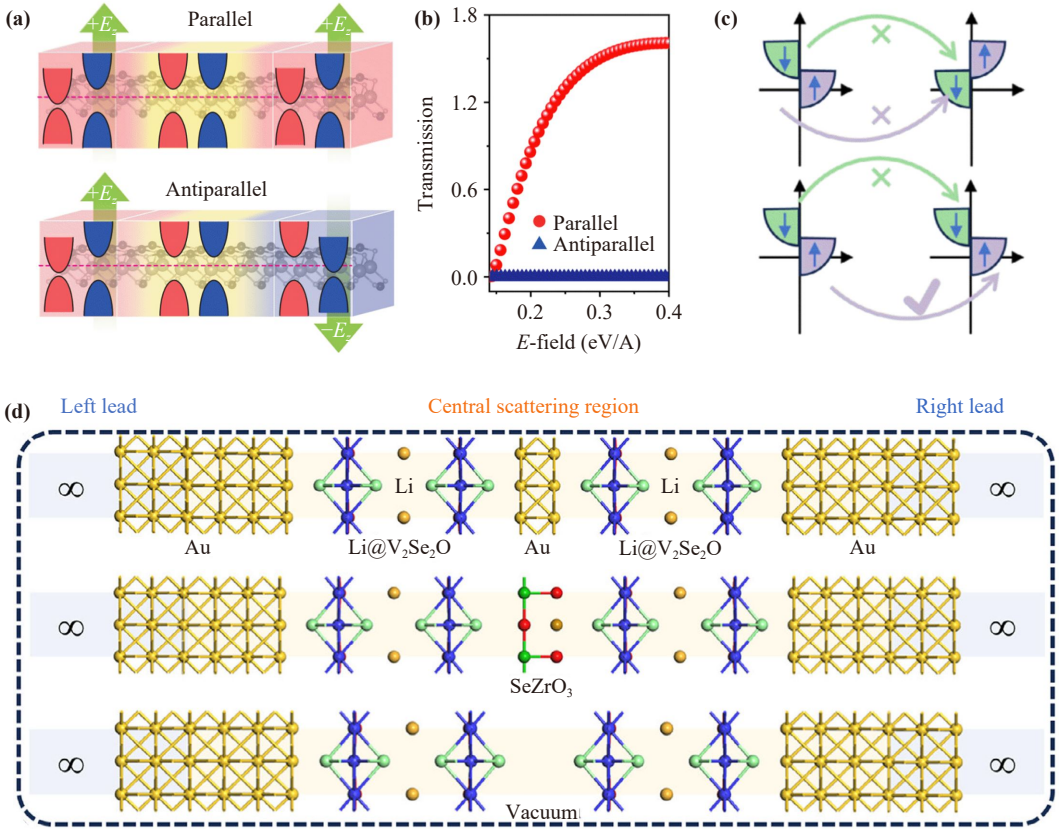

Fig. 11 **(a)** Parallel and antiparallel configurations of the giant tunneling magnetoresistance TMR-like device based on AMFV materials [59]. **(b)** Total transmission as a function of E_z for the $Ca(CoN)_2$ tunnel junction [59]. **(c)** Illustration of the tunneling process based on calculated density of states, for antiparallel and parallel states [160]. **(d)** The V_2Se_2O-based magnetoresistance devices with an electrode of Au and intermediate layers of Au, $SrZrO_3$ or vacuum [160].

field of ~10^3 T and realizes complete spin/valley current switching (ON/OFF ratio for spin current approaching 100%) [Fig. 11(a)]. When electric fields are applied to both electrodes, the polarization states align, and the device exhibits a low-resistance state. Conversely, when opposite electric fields are applied, the device switches to a high-resistance state with a giant tunneling magnetoresistance (TMR) effect [Fig. 11(b)] [59]. Electron transport is feasible between valleys contributing the same spin, but not between valleys with different spins [Fig. 11(c)]. Notably, the compound KV_2Se_2O was successfully synthesized via the self-flux method (with KSe as flux agent, sintered at 1000 ℃ and slowly cooled at 2 K/h) , and it has been confirmed to be a room-temperature metallic altermagnet with *d*-wave spin-momentum locking [163]. If monolayer V_2Se_2O can be exfoliated from its parent compound KV_2Se_2O, it will provide direct experimental evidence for the application of V_2Se_2O monolayers in high-performance devices. Furthermore, through intercalation modification (Li or V intercalation), V_2Se_2O bilayer can exhibit ferrimagnetic-ferroelastic characteristics and a half-metallic electronic structure at above room temperature (Li: 358 K, V: 773 K), with magnetic order dynamics and no performance degradation during device operation at ambient temperature (300 K) device operation, and the ferroelastic switching barrier (0.202–0.210 eV) ensures long-term retention stability of the device state (thermal disturbance resistance at 300 K). Spintronic devices constructed from this intercalated V_2Se_2O bilayer achieve a giant magnetoresistance (GMR) of up to 877% (V-intercalated) and an ultrahigh thermal tunneling magnetoresistance of nearly 12000% under finite-temperature gradient conditions, which is two to three orders of magnitude higher than the thermal TMR of traditional 2D magnetic spintronic devices (typically < 100%) [Fig. 11(d)]. The Li-intercalated V_2Se_2O system can become a metallic phase with enhanced spin splitting, while the V-intercalated system changes to a half-metallic phase with nearly 100% spin-filtering efficiency (96%–98% at equilibrium), maintaining high spin polarization stability against finite-temperature fluctuations, and the latter enables nearly perfect spin-filtering efficiency [160]. Overall, the AMFV systems systematically address key challenges in generating, manipulating, detecting, and retaining valley information. This transitions valleytronics from a laboratory phenomenon to a developmental stage geared towards room-temperature

operation, all-electrical control, and high-density integration, showing transformative potential for next-generation information devices.

6 Challenges and outlook

Although AMFV materials exhibit transformative potential in theory, their journey from concept to application faces a series of pressing key challenges. Currently, the most significant bottleneck lies in the extreme scarcity of material systems. Most candidates (e.g., V_2Se_2O, $Ca(CoN)_2$ and Fe_2MX_4) remain at the stage of theoretical calculations, with very few experimentally verifiable samples available, making it difficult to confirm their key physical properties. For instance, while bulk parent compound KV_2Se_2O has been experimentally synthesized, fabricating high-quality monolayer V_2Se_2O films remain challenging. This gap prevents experimental validation of key physical parameters, particularly the intrinsic spin-valley locking strength. Another fundamental challenge is the lack of a dedicated symmetry and group-theoretical framework for AMFV systems. Conventional magnetic space groups are insufficient to describe altermagnetic order, which requires spin-space groups for proper classification. However, no unified symmetry principles or group-theoretical classification schemes capable of simultaneously describing altermagnetic order and valley polarization have been established for AMFV materials. The roles of nonsymmorphic symmetries and anti-unitary operations in governing spin-valley locking and valley polarization also remain largely unexplored. Furthermore, the underlying physical mechanisms are still unclear. There is a lack of a unified theoretical framework for the complex multiferroic coupling between AMFV and other ferroic orders (such as FE and FA), as well as for the mutual regulation among multiple degrees of freedom (electron, spin, valley, optical and layer), which severely hinders the targeted design and performance modulation of such materials. Ultimately, device-oriented applications remains largely unexplored. How to translate their unique properties into feasible prototype devices (e.g., valley tunnel junctions, valley filters and high-density memories) and address key issues such as electrical writing, reading, and integration remains largely uncharted territory. Although electrically controlled tunnel junctions based on $Ca(CoN)_2$ have been proposed, there is still no experimental verification of low-power electrically controlled switching of VP.

To overcome these obstacles, future research should be strategically directed toward several key directions. First, revolutionizing material discovery and synthesis by utilizing high-throughput calculations and machine learning to expand the candidate library beyond current 2D systems (e.g., 2D wurtzite multiferroics, metal–organic frameworks), and combining this with advanced growth and characterization techniques to prepare high-quality samples, thereby constructing a reliable experimental material database. Second, establish symmetry-based design rules and group-theoretical classifications for AMFV materials, including the analysis of nonsymmorphic symmetries and anti-unitary operations, to enable rational material design. Third, deepen the understanding of the microscopic mechanisms by employing multi-scale theoretical modeling to elucidate the coupling mechanisms of multiple degrees of freedom. Specifically, focus on developing experimental strategies to verify SOC-independent valley splitting, thereby clarifying the physical origins. Finally, prioritize the development of device principles and integration by exploring compatible pathways campatible CMOS processes and novel spintronic architectures, starting with the development of unit devices such as electrically or mechanically controlled valley switches, to gradually promote their translation into practical applications.

7 Conclusion

In summary, the emergence of AMFV materials marks a critical paradigm shift in valleytronics This shift moves beyond a heavy reliance on intrinsic strong SOC toward the active utilization of synergistic design between altermagnetic order and crystal symmetry to generate and manipulate valley degrees of freedom. Such materials provide a new physical foundation and a versatile material platform to overcome long-standing bottlenecks in traditional valleytronic devices, including room-temperature operation, full electrical control, high-density integration, and low-power consumption. Theoretical studies have outlined multiple promising pathways — from V_2Se_2O to Fe_2MX_4 systems — and demonstrated efficient tuning of VP via strain, electric fields, sliding, twisting and proximity effects, yet translating this potential into practical technology remains constrained by multiple challenges in material preparation, mechanism understanding, and device implementation. Future progress will hinge on deeper integration among computational design, advanced characterization, material synthesis, and nanofabrication. Overcoming these challenges could not only enable novel information devices that transcend the limits of Moore's Law but also establish a new research paradigm in which symmetry engineering harnesses intrinsic electronic degrees of freedom.

Declarations The authors declare no competing financial interest.

Acknowledgements This work was supported by the National Key Research and Development Program of China (Grant No. 2022YFA1402902), the National Natural Science Foundation of China (Grant Nos. 12134003, 12304218, 125B2069, and 62374002), Shanghai Science and Technology Innovation Action Plan (Grant No.

21JC1402000), Shanghai Pujiang Program (Grant No. 23PJ1402200), the Research Fund of the Suzhou National Laboratory (Grant No. SK-1202-2024-012), ECNU Academic Innovation Promotion Program for Excellent Doctoral Students (No. YBNLTS2025-025), and East China Normal University Multifunctional Platform for Innovation (001 and 006).

References

1. J. Lee, Z. Wang, H. Xie, K. F. Mak, and J. Shan, Valley magnetoelectricity in single-layer MoS_2, *Nat. Mater.* 16(9), 887 (2017)
2. H. K. Li, K. Y. Fong, H. Zhu, Q. Li, S. Wang, S. Yang, Y. Wang, and X. Zhang, Valley optomechanics in a monolayer semiconductor, *Nat. Photonics* 13(6), 397 (2019)
3. Y. C. Wu, T. Taniguchi, K. Watanabe, and J. Yan, Valley polarized holes induced exciton polaron valley splitting, *ACS Nano* 17(16), 15641 (2023)
4. S. Zhao, X. Li, B. Dong, H. Wang, H. Wang, Y. Zhang, Z. Han, and H. Zhang, Valley manipulation in monolayer transition metal dichalcogenides and their hybrid systems: Status and challenges, *Rep. Prog. Phys.* 84(2), 026401 (2021)
5. N. M. Freitag, T. Reisch, L. A. Chizhova, P. Nemes-Incze, C. Holl, C. R. Woods, R. V. Gorbachev, Y. Cao, A. K. Geim, K. S. Novoselov, J. Burgdörfer, F. Libisch, and M. Morgenstern, Large tunable valley splitting in edge-free graphene quantum dots on boron nitride, *Nat. Nanotechnol.* 13(5), 392 (2018)
6. I. Tyulnev, Á. Jiménez-Galán, J. Poborska, L. Vamos, P. S. J. Russell, F. Tani, O. Smirnova, M. Ivanov, R. E. F. Silva, and J. Biegert, Valleytronics in bulk MoS_2 with a topologic optical field, *Nature* 628(8009), 746 (2024)
7. K. S. Novoselov, A. K. Geim, S. V. Morozov, D. Jiang, Y. Zhang, S. V. Dubonos, I. V. Grigorieva, and A. A. Firsov, Electric field effect in atomically thin carbon films, *Science* 306(5696), 666 (2004)
8. D. Xiao, W. Yao, and Q. Niu, Valley-contrasting physics in graphene: Magnetic moment and topological transport, *Phys. Rev. Lett.* 99(23), 236809 (2007)
9. J. R. Schaibley, H. Yu, G. Clark, P. Rivera, J. S. Ross, K. L. Seyler, W. Yao, and X. Xu, Valleytronics in 2D materials, *Nat. Rev. Mater.* 1(11), 16055 (2016)
10. N. Singh and U. Schwingenschlögl, A route to permanent valley polarization in monolayer MoS_2, *Adv. Mater.* 29(1), 1600970 (2017)
11. Z. Zhu, A. Collaudin, B. Fauqué, W. Kang, and K. Behnia, Field-induced polarization of Dirac valleys in bismuth, *Nat. Phys.* 8(1), 89 (2012)
12. F. Zhang, J. Jung, G. A. Fiete, Q. Niu, and A. H. MacDonald, Spontaneous quantum Hall states in chirally stacked few-layer graphene systems, *Phys. Rev. Lett.* 106(15), 156801 (2011)
13. T. Cao, G. Wang, W. Han, H. Ye, C. Zhu, J. Shi, Q. Niu, P. Tan, E. Wang, B. Liu, and J. Feng, Valley-selective circular dichroism of monolayer molybdenum disulphide, *Nat. Commun.* 3(1), 887 (2012)
14. T. Smoleński, M. Goryca, M. Koperski, C. Faugeras, T. Kazimierczuk, A. Bogucki, K. Nogajewski, P. Kossacki, and M. Potemski, Tuning valley polarization in a WSe_2 monolayer with a tiny magnetic field, *Phys. Rev. X* 6(2), 021024 (2016)
15. D. J. Shin, H. Cho, J. Sung, and S. H. Gong, Direct observation of self-hybridized exciton-polaritons and their valley polarizations in a bare WS_2 layer, *Adv. Mater.* 34(50), 2207735 (2022)
16. L. Chen, Z. Li, Q. Li, Q. Zheng, and J. Zhao, Spin valley dynamics entangled with optical fields, phonons, and spin-orbit coupling in monolayer MoSe2, *Adv. Opt. Mater.* 13(11), 2403069 (2025)
17. J. D. Zheng, Y. F. Zhao, Y. F. Tan, Z. Guan, N. Zhong, F. Y. Yue, P. H. Xiang, and C. G. Duan, Coupling of ferroelectric and valley properties in 2D materials, *J. Appl. Phys.* 132(12), 120902 (2022)
18. W. Y. Tong, S. J. Gong, X. Wan, and C. G. Duan, Concepts of ferrovalley material and anomalous valley Hall effect, *Nat. Commun.* 7(1), 13612 (2016)
19. K. Sheng, Q. Chen, H. K. Yuan, and Z. Y. Wang, Monolayer CeI_2: An intrinsic room-temperature ferrovalley semiconductor, *Phys. Rev. B* 105(7), 075304 (2022)
20. Y. Wu, J. Tong, L. Deng, F. Luo, F. Tian, G. Qin, and X. Zhang, Coexisting ferroelectric and ferrovalley polarizations in bilayer stacked magnetic semiconductors, *Nano Lett.* 23(13), 6226 (2023)
21. S. D. Guo, Y. L. Tao, W. Q. Mu, and B. G. Liu, Correlation-driven threefold topological phase transition in monolayer $OsBr_2$, *Front. Phys. (Beijing)* 18(3), 33304 (2023)
22. K. Sheng, B. Zhang, and Z. Y. Wang, Valley polarization in a two-dimensional high-temperature semiconducting $TiInTe_3$ honeycomb ferromagnet, *Acta Mater.* 262, 119461 (2024)
23. G. Zheng, S. Qu, W. Zhou, and F. Ouyang, Janus monolayer TaNF: A new ferrovalley material with large valley splitting and tunable magnetic properties, *Front. Phys. (Beijing)* 18(5), 53302 (2023)
24. K. Sheng, B. Zhang, H. K. Yuan, and Z. Y. Wang, Strain-engineered topological phase transitions in ferrovalley 2H-$RuCl_2$ monolayer, *Phys. Rev. B* 105(19), 195312 (2022)
25. S. D. Guo, W. Q. Mu, J. H. Wang, Y. X. Yang, B. Wang, and Y. S. Ang, Strain effects on the topological and valley properties of the Janus monolayer $VSiGeN_4$, *Phys. Rev. B* 106(6), 064416 (2022)
26. J. D. Zheng, Y. F. Zhao, Z. Q. Bao, Y. H. Shen, Z. Guan, N. Zhong, F. Y. Yue, P. H. Xiang, and C. G. Duan, Flexoelectric effect induced p–n homojunction in monolayer GeSe, *2D Mater.* 9(3), 035005 (2022)
27. Y. Q. Li, X. Zhang, X. Shang, Q. W. He, D. S. Tang, X. C. Wang, and C. G. Duan, Magnetic and ferroelectric manipulation of valley physics in janus piezoelectric materials, *Nano Lett.* 23(21), 10013 (2023)
28. C. Zhang, Y. Nie, S. Sanvito, and A. Du, First-principles prediction of a room-temperature ferromagnetic Janus VSSe monolayer with piezoelectricity, ferroelasticity, and large valley polarization, *Nano Lett.* 19(2), 1366 (2019)

29. P. Man, L. Huang, J. Zhao, and T. H. Ly, Ferroic phases in two-dimensional materials, *Chem. Rev.* 123(18), 10990 (2023)
30. Y. Liu, Y. Feng, Y. Dai, B. Huang, and Y. Ma, Ferrovalleytricity with in-plane spin magnetization, *Nano Lett.* 25(2), 762 (2025)
31. J. Chu, Y. Wang, X. Wang, K. Hu, G. Rao, C. Gong, C. Wu, H. Hong, X. Wang, K. Liu, C. Gao, and J. Xiong, 2D polarized materials: ferromagnetic, ferrovalley, ferroelectric materials, and related heterostructures, *Adv. Mater.* 33(5), 2004469 (2021)
32. Y. F. Zhao, Y. H. Shen, H. Hu, W. Y. Tong, and C. G. Duan, Combined piezoelectricity and ferrovalley properties in Janus monolayer VClBr, *Phys. Rev. B* 103(11), 115124 (2021)
33. Z. Zhou, H. Wang, and X. Li, Multiple valley modulations in noncollinear antiferromagnets, *Nano Lett.* 24(37), 11497 (2024)
34. Y. Feng, S. Qi, Y. Ren, M. Liu, N. Liu, M. Liu, Q. Yang, and S. Meng, Prediction of intrinsic multiferroicity and large valley polarization in a layered Janus material, *npj Comput. Mater.* 11(1), 264 (2025)
35. Y. Liu, Y. Feng, T. Zhang, Z. He, Y. Dai, B. Huang, and Y. Ma, Strain-valley coupling in 2D antiferromagnetic lattice, *Adv. Funct. Mater.*, doi: 10.1002/adfm.202305130 (2023)
36. Y. K. Zhang, J. D. Zheng, W. Y. Tong, Y. F. Zhao, Y. F. Tan, Y. H. Shen, Z. Guan, F. Y. Yue, P. H. Xiang, N. Zhong, J. H. Chu, and C. G. Duan, Ferroelastically controlled ferrovalley states in stacked bilayer systems with inversion symmetry, *Phys. Rev. B* 108(24), L241120 (2023)
37. G. Yu, J. Ji, C. Xu, and H. J. Xiang, Bilayer stacking ferrovalley materials without breaking time-reversal and spatial-inversion symmetry, *Phys. Rev. B* 109(7), 075434 (2024)
38. L. Šmejkal, J. Sinova, and T. Jungwirth, Beyond conventional ferromagnetism and antiferromagnetism: A phase with nonrelativistic spin and crystal rotation symmetry, *Phys. Rev. X* 12(3), 031042 (2022)
39. L. Šmejkal, J. Sinova, and T. Jungwirth, Emerging research landscape of altermagnetism, *Phys. Rev. X* 12(4), 040501 (2022)
40. Z. Guo, X. Wang, W. Wang, G. Zhang, X. Zhou, and Z. Cheng, Spin-polarized antiferromagnets for spintronics, *Adv. Mater.* 37(36), 2505779 (2025)
41. L. Bai, W. Feng, S. Liu, L. Šmejkal, Y. Mokrousov, and Y. Yao, Altermagnetism: Exploring new frontiers in magnetism and spintronics, *Adv. Funct. Mater.* 34(49), 2409327 (2024)
42. S. W. Cheong and F. T. Huang, Altermagnetism with non-collinear spins, *npj Quantum Mater.* 9(1), 13 (2024)
43. J. Ding, Z. Jiang, X. Chen, Z. Tao, Z. Liu, T. Li, J. Liu, J. Sun, J. Cheng, J. Liu, Y. Yang, R. Zhang, L. Deng, W. Jing, Y. Huang, Y. Shi, M. Ye, S. Qiao, Y. Wang, Y. Guo, D. Feng, and D. Shen, Large band splitting in g-wave altermagnet CrSb, *Phys. Rev. Lett.* 133(20), 206401 (2024)
44. Y. X. Li and C. C. Liu, Majorana corner modes and tunable patterns in an altermagnet heterostructure, *Phys. Rev. B* 108(20), 205410 (2023)
45. S. A. A. Ghorashi, T. L. Hughes, and J. Cano, Altermagnetic routes to Majorana modes in zero net magnetization, *Phys. Rev. Lett.* 133(10), 106601 (2024)
46. L. Šmejkal, R. González-Hernández, T. Jungwirth, and J. Sinova, Crystal time-reversal symmetry breaking and spontaneous Hall effect in collinear antiferromagnets, *Sci. Adv.* 6(23), eaaz8809 (2024)
47. X. Zhou, W. Feng, R. W. Zhang, L. Šmejkal, J. Sinova, Y. Mokrousov, and Y. Yao, Crystal thermal transport in altermagnetic RuO_2, *Phys. Rev. Lett.* 132(5), 056701 (2024)
48. T. Osumi, S. Souma, T. Aoyama, K. Yamauchi, A. Honma, K. Nakayama, T. Takahashi, K. Ohgushi, and T. Sato, Observation of a giant band splitting in altermagnetic MnTe, *Phys. Rev. B* 109(11), 115102 (2024)
49. J. Krempaský, L. Šmejkal, S. W. D'Souza, M. Hajlaoui, G. Springholz, K. Uhlířová, F. Alarab, P. C. Constantinou, V. Strocov, D. Usanov, W. R. Pudelko, R. González-Hernández, A. Birk Hellenes, Z. Jansa, H. Reichlová, Z. Šobáň, R. D. G. Betancourt, P. Wadley, J. Sinova, D. Kriegner, J. Minár, J. H. Dil, and T. Jungwirth, Altermagnetic lifting of Kramers spin degeneracy, *Nature* 626(7999), 517 (2024)
50. H. Bai, Y. C. Zhang, Y. J. Zhou, P. Chen, C. H. Wan, L. Han, W. X. Zhu, S. X. Liang, Y. C. Su, X. F. Han, F. Pan, and C. Song, Efficient spin-to-charge conversion via altermagnetic spin splitting effect in antiferromagnet RuO_2, *Phys. Rev. Lett.* 130(21), 216701 (2023)
51. C. Song, H. Bai, Z. Zhou, L. Han, H. Reichlova, J. H. Dil, J. Liu, X. Chen, and F. Pan, Altermagnets as a new class of functional materials, *Nat. Rev. Mater.* 10(6), 473 (2025)
52. F. Zhang, X. Cheng, Z. Yin, C. Liu, L. Deng, Y. Qiao, Z. Shi, S. Zhang, J. Lin, Z. Liu, M. Ye, Y. Huang, X. Meng, C. Zhang, T. Okuda, K. Shimada, S. Cui, Y. Zhao, G. H. Cao, S. Qiao, J. Liu, and C. Chen, Crystal-symmetry-paired spin–valley locking in a layered room-temperature metallic altermagnet candidate, *Nat. Phys.* 21(5), 760 (2025)
53. M. G. Cuxart, R. Robles, B. Muñiz Cano, P. Gargiani, C. Rebanal, I. Di Bernardo, A. Amiri, F. Calleja, M. Garnica, M. A. Valbuena, and A. L. Vázquez de Parga, Emergent magnetic structures at the 2D limit of the altermagnet MnTe, *Adv. Funct. Mater.*, doi: 10.1002/adfm.202516924 (2025)
54. M. Liu, J. T. Sun, and S. Meng, Uncompensated linear dichroism of magneto-optical Kerr effect in a 2D altermagnet, *Adv. Funct. Mater.*, doi: 10.1002/adfm.202521111 (2026)
55. J. Wang, X. Yang, Z. Yang, J. Lu, P. Ho, W. Wang, Y. S. Ang, Z. Cheng, and S. Fang, Pentagonal 2D altermagnets: Material screening and altermagnetic tunneling junction device application, *Adv. Funct. Mater.*, doi: 10.1002/adfm.202505145 (2026)
56. L. Camerano, A. O. Fumega, J. L. Lado, A. Stroppa, and G. Profeta, Multiferroic nematic d-wave altermagnetism driven by orbital-order on the honeycomb lattice, *npj 2D Mater. Appl.* 9(1), 75 (2025)
57. H. Y. Ma, M. Hu, N. Li, J. Liu, W. Yao, J. F. Jia, and J. Liu, Multifunctional antiferromagnetic materials

with giant piezomagnetism and noncollinear spin current, *Nat. Commun.* 12(1), 2846 (2021)
58. Y. Zhu, T. Chen, Y. Li, L. Qiao, X. Ma, C. Liu, T. Hu, H. Gao, and W. Ren, Multipiezo effect in altermagnetic V_2SeTeO monolayer, *Nano Lett.* 24(1), 472 (2024)
59. R. W. Zhang, C. Cui, R. Li, J. Duan, L. Li, Z. M. Yu, and Y. Yao, Predictable gate-field control of spin in altermagnets with spin-layer coupling, *Phys. Rev. Lett.* 133(5), 056401 (2024)
60. C. Y. Tan, Z. F. Gao, H. C. Yang, Z. X. Liu, K. Liu, P. J. Guo, and Z. Y. Lu, Crystal valley Hall effect, *Phys. Rev. B* 111(9), 094411 (2025)
61. D. Xiao, G. B. Liu, W. Feng, X. Xu, and W. Yao, Coupled spin and valley physics in monolayers of MoS_2 and other group-VI dichalcogenides, *Phys. Rev. Lett.* 108(19), 196802 (2012)
62. Y. Ma, Y. Wu, J. Tong, L. Deng, X. Yin, L. Zhou, X. Han, F. Tian, and X. Zhang, Distinct ferrovalley characteristics of the Janus RuClX (X = F, Br) monolayer, *Nanoscale* 15(18), 8278 (2023)
63. Y. Zang, Y. Ma, R. Peng, H. Wang, B. Huang, and Y. Dai, Large valley-polarized state in single-layer NbX_2 (X = S, Se): Theoretical prediction, *Nano Res.* 14(3), 834 (2021)
64. W. Y. Tong and C. G. Duan, Electrical control of the anomalous valley Hall effect in antiferrovalley bilayers, *npj Quantum Mater.* 2(1), 47 (2017)
65. H. Hu, W. Y. Tong, Y. H. Shen, X. Wan, and C. G. Duan, Concepts of the half-valley-metal and quantum anomalous valley Hall effect, *npj Comput. Mater.* 6(1), 129 (2020)
66. M. Tian, C. Cui, Z. Li, Z. M. Yu, and R. W. Zhang, Switchable valley-contrasting Berry curvature in two-dimensional valley-semi-half-metals, *Phys. Rev. B* 112(4), 045144 (2025)
67. H. Huan, Y. Xue, B. Zhao, G. Gao, H. Bao, and Z. Yang, Strain-induced half-valley metals and topological phase transitions in MBr_2 monolayers (M = Ru, Os), *Phys. Rev. B* 104(16), 165427 (2021)
68. S. D. Guo, Y. L. Tao, G. Wang, S. Chen, D. Huang, and Y. S. Ang, Proposal for valleytronic materials: Ferrovalley metal and valley gapless semiconductor, *Front. Phys. (Beijing)* 19(2), 23302 (2023)
69. Y. K. Zhang, J. D. Zheng, Y. H. Shen, Y. F. Zhao, Y. Q. Li, Z. Q. Bao, W. Y. Tong, J. H. Chu, and C. G. Duan, Electric-field-induced quantum anomalous valley Hall effect in antiferromagnetic bilayer, *Newton* 1(8), 100205 (2025)
70. Y. Feng and Q. Yang, Enabling triferroics coupling in breathing kagome lattice Nb_3X_8 (X = Cl, Br, I) monolayers, *J. Mater. Chem. C* 11(17), 5762 (2023)
71. Z. Zhang, H. Huang, Y. Zhao, L. Wang, C. Liu, S. Zhou, Y. Wu, J. Zhao, G. Qiao, J. Zhang, X. Zheng, and S. Wang, Nonvolatile ferroelectric manipulation of topological states in two-dimensional multiferroic van der Waals heterostructures, *ACS Nano* 19(20), 18976 (2025)
72. H. Hu, W. Y. Tong, Y. H. Shen, and C. G. Duan, Electrical control of the valley degree of freedom in 2D ferroelectric/antiferromagnetic heterostructures, *J. Mater. Chem. C* 8(24), 809 (2020)
73. Y. Feng, J. Zhao, Y. Dai, B. Huang, and Y. Ma, Atypical breathing driven two-dimensional valley multiferroicity, *Mater. Horiz.* 11(24), 6391 (2024)
74. K. Q. Wang, J. D. Zheng, W. Y. Tong, and C. G. Duan, Breathing ferroelectricity induced topological valley states in kagome niobium halide monolayers, *npj Comput. Mater.* 11(1), 223 (2025)
75. J. Ma, X. Luo, and Y. Zheng, Strain engineering the spin-valley coupling of the R-stacking sliding ferroelectric bilayer 2H-VX_2 (X = S, Se, Te), *npj Comput. Mater.* 10(1), 102 (2024)
76. T. Zhong, Y. Ren, Z. Zhang, J. Gao, and M. Wu, Sliding ferroelectricity in two-dimensional MoA_2N_4 (A = Si or Ge) bilayers: High polarizations and moiré potentials, *J. Mater. Chem. A* 9(35), 19659 (2021)
77. E. Y. Tsymbal, Two-dimensional ferroelectricity by design, *Science* 372(6549), 1389 (2021)
78. X. Liu, A. P. Pyatakov, and W. Ren, Magnetoelectric coupling in multiferroic bilayer VS_2, *Phys. Rev. Lett.* 125(24), 247601 (2020)
79. L. Liang, Y. Yang, X. Wang, and X. Li, Tunable valley and spin splittings in VSi_2N_4 bilayers, *Nano Lett.* 23(3), 858 (2023)
80. L. Zhang, Y. Liu, M. Wu, and G. Gao, Electric-field- and stacking-tuned antiferromagnetic FeClF bilayer: The coexistence of bipolar magnetic semiconductor and anomalous valley Hall effect, *Adv. Funct. Mater.* 35(17), 2417857 (2025)
81. C. Wu, H. Sun, P. Dong, Y. Z. Wu, and P. Li, Coexisting triferroic and multiple types of valley polarization by structural phase transition in 2D materials, *Adv. Funct. Mater.* 35(31), 2501506 (2025)
82. S. Park, S. Arscott, T. Taniguchi, K. Watanabe, F. Sirotti, and F. Cadiz, Efficient valley polarization of charged excitons and resident carriers in molybdenum disulfide monolayers by optical pumping, *Commun. Phys.* 5(1), 73 (2022)
83. K. Shao, H. Geng, E. Liu, J. L. Lado, W. Chen, and D. Y. Xing, Non-Hermitian moiré valley filter, *Phys. Rev. Lett.* 132(15), 156301 (2024)
84. L. Li, L. Shao, X. Liu, A. Gao, H. Wang, B. Zheng, G. Hou, K. Shehzad, L. Yu, F. Miao, Y. Shi, Y. Xu, and X. Wang, Room-temperature valleytronic transistor, *Nat. Nanotechnol.* 15(9), 743 (2020)
85. R. Liu, Y. Zhang, Y. Zhou, J. Nie, L. Li, and Y. Zhang, Polarization-driven high Rabi frequency of piezotronic valley transistors, *Nano Energy* 113, 108550 (2023)
86. D. Dai, B. Fu, J. Yang, L. Yang, S. Yan, et al., Twist angle–dependent valley polarization switching in heterostructures, *Sci. Adv.* 10(20), eado1281 (2025)
87. P. Rivera, K. L. Seyler, H. Yu, J. R. Schaibley, J. Yan, D. G. Mandrus, W. Yao, and X. Xu, Valley-polarized exciton dynamics in a 2D semiconductor heterostructure, *Science* 351(6274), 688 (2016)
88. W. Zhou, G. Zheng, Z. Wan, T. Sun, A. Li, and F. Ouyang, Valley-dependent topological phase transition in monolayer ferrovalley materials RuXY (X, Y = F, Cl, Br), *Appl. Phys. Lett.* 123(14), 143101 (2023)
89. Y. Liu, Y. Gao, S. Zhang, J. He, J. Yu, and Z. Liu,

Valleytronics in transition metal dichalcogenides materials, *Nano Res.* 12(11), 2695 (2019)
90. R. Xu, Z. Zhang, J. Liang, and H. Zhu, Valleytronics: Fundamental challenges and materials beyond transition metal chalcogenides, *Small* 21(28), 2402139 (2025)
91. Y. Y. Jiang, Z. A. Wang, K. Samanta, S. H. Zhang, R. C. Xiao, W. J. Lu, Y. P. Sun, E. Y. Tsymbal, and D. F. Shao, Prediction of giant tunneling magnetoresistance in $RuO_2/TiO_2/RuO_2$ (110) antiferromagnetic tunnel junctions, *Phys. Rev. B* 108(17), 174439 (2023)
92. S. B. Zhang, L. H. Hu, and T. Neupert, Finite-momentum Cooper pairing in proximitized altermagnets, *Nat. Commun.* 15(1), 1801 (2024)
93. S. Bhowal and N. A. Spaldin, Ferroically ordered magnetic octupoles in *d*-wave altermagnets, *Phys. Rev. X* 14(1), 011019 (2024)
94. L. Šmejkal, A. H. MacDonald, J. Sinova, S. Nakatsuji, and T. Jungwirth, Anomalous Hall antiferromagnets, *Nat. Rev. Mater.* 7(6), 482 (2022)
95. R. D. Gonzalez Betancourt, J. Zubáč, R. Gonzalez-Hernandez, K. Geishendorf, Z. Šobáň, G. Springholz, K. Olejník, L. Šmejkal, J. Sinova, T. Jungwirth, S. T. B. Goennenwein, A. Thomas, H. Reichlová, J. Železný, and D. Kriegner, Spontaneous anomalous Hall effect arising from an unconventional compensated magnetic phase in a semiconductor, *Phys. Rev. Lett.* 130(3), 036702 (2023)
96. X. Feng, H. Bai, X. Fan, M. Guo, Z. Zhang, G. Chai, T. Wang, D. Xue, C. Song, and X. Fan, Incommensurate spin density wave in antiferromagnetic RuO_2 evinced by abnormal spin splitting torque, *Phys. Rev. Lett.* 132(8), 086701 (2024)
97. O. E. Parfenov, D. V. Averyanov, I. S. Sokolov, A. N. Mihalyuk, O. A. Kondratev, A. N. Taldenkov, A. M. Tokmachev, and V. G. Storchak, Scaling the altermagnet GdAlSi beyond the monolayer limit, *J. Am. Chem. Soc.* 147(27), 23857 (2025)
98. H. J. Lin, S. B. Zhang, H. Z. Lu, and X. C. Xie, Coulomb drag in altermagnets, *Phys. Rev. Lett.* 134(13), 136301 (2025)
99. R. B. Regmi, H. Bhandari, B. Thapa, Y. Hao, N. Sharma, J. McKenzie, X. Chen, A. Nayak, M. El Gazzah, B. G. Márkus, L. Forró, X. Liu, H. Cao, J. F. Mitchell, I. I. Mazin, and N. J. Ghimire, Altermagnetism in the layered intercalated transition metal dichalcogenide $CoNb_4Se_8$, *Nat. Commun.* 16(1), 4399 (2025)
100. H. C. Mandujano, S. Sheoran, Y. Zhang, T. Li, S. J. Hong, P. Dev, and E. E. Rodriguez, Evolution of altermagnetism to spin density waves in Co_xNbSe_2, *J. Am. Chem. Soc.* 147(49), 44926 (2025)
101. X. Zhang, P. Jiang, L. Y. Xu, L. Wang, L. Liu, H. M. Huang, T. Cao, and Y. L. Li, Giant spin splitting and anisotropic spin polarization in 2D altermagnet Cr_2O, *Nano Lett.* 25(46), 16547 (2025)
102. S. Lee, S. Lee, S. Jung, J. Jung, D. Kim, Y. Lee, B. Seok, J. Kim, B. G. Park, L. Šmejkal, C. J. Kang, and C. Kim, Broken Kramers degeneracy in altermagnetic MnTe, *Phys. Rev. Lett.* 132(3), 036702 (2024)
103. Y. P. Zhu, X. Chen, X. R. Liu, Y. Liu, P. Liu, H. Zha, G. Qu, C. Hong, J. Li, Z. Jiang, X. M. Ma, Y. J. Hao, M. Y. Zhu, W. Liu, M. Zeng, S. Jayaram, M. Lenger, J. Ding, S. Mo, K. Tanaka, M. Arita, Z. Liu, M. Ye, D. Shen, J. Wrachtrup, Y. Huang, R. H. He, S. Qiao, Q. Liu, and C. Liu, Observation of plaid-like spin splitting in a noncoplanar antiferromagnet, *Nature* 626(7999), 523 (2024)
104. S. Reimers, L. Odenbreit, L. Šmejkal, V. N. Strocov, P. Constantinou, A. B. Hellenes, R. Jaeschke Ubiergo, W. H. Campos, V. K. Bharadwaj, A. Chakraborty, T. Denneulin, W. Shi, R. E. Dunin-Borkowski, S. Das, M. Kläui, J. Sinova, and M. Jourdan, Direct observation of altermagnetic band splitting in CrSb thin films, *Nat. Commun.* 15(1), 2116 (2024)
105. I. J. Park, S. Kwon, and R. K. Lake, Effects of filling, strain, and electric field on the Néel vector in antiferromagnetic CrSb, *Phys. Rev. B* 102(22), 224426 (2020)
106. Q. Liu, J. Kang, P. Wang, W. Gao, Y. Qi, J. Zhao, and X. Jiang, Inverse magnetocaloric effect in altermagnetic 2D non-van der Waals FeX (X = S and Se) semiconductors, *Adv. Funct. Mater.*, doi: 10.1002/adfm.202402080 (2024)
107. H. Bai, Y. C. Zhang, Y. J. Zhou, P. Chen, C. H. Wan, L. Han, W. X. Zhu, S. X. Liang, Y. C. Su, X. F. Han, F. Pan, and C. Song, Efficient spin-to-charge conversion via altermagnetic spin splitting effect in antiferromagnet RuO_2, *Phys. Rev. Lett.* 130(21), 216701 (2023)
108. H. Bai, L. Han, X. Y. Feng, Y. J. Zhou, R. X. Su, Q. Wang, L. Y. Liao, W. X. Zhu, X. Z. Chen, F. Pan, X. L. Fan, and C. Song, Observation of spin splitting torque in a collinear antiferromagnet RuO_2, *Phys. Rev. Lett.* 128(19), 197202 (2022)
109. X. Zhu, X. Huo, S. Feng, S. B. Zhang, S. A. Yang, and H. Guo, Design of altermagnetic models from spin clusters, *Phys. Rev. Lett.* 134(16), 166701 (2025)
110. Z. M. Wang, Y. Zhang, S. B. Zhang, J. H. Sun, E. Dagotto, D. H. Xu, and L. H. Hu, Spin-orbital altermagnetism, *Phys. Rev. Lett.* 135(17), 176705 (2025)
111. M. Pan, F. Liu, and H. Huang, Orbital altermagnetism, arXiv: 2510.00509 (2025)
112. D. Dey, S. Choudhary, S. Ramasesha, and R. Raghunathan, Charge-order-driven altermagnetism in a bipartite lattice, *Phys. Rev. B* 111(21), 214439 (2025)
113. M. Gu, Y. Liu, H. Zhu, K. Yananose, X. Chen, Y. Hu, A. Stroppa, and Q. Liu, Ferroelectric switchable altermagnetism, *Phys. Rev. Lett.* 134(10), 106802 (2025)
114. X. Duan, J. Zhang, Z. Zhu, Y. Liu, Z. Zhang, I. Žutić, and T. Zhou, Antiferroelectric altermagnets: Antiferroelectricity alters magnets, *Phys. Rev. Lett.* 134(10), 106801 (2025)
115. R. Peng, S. Fang, P. Ho, T. Zhou, J. Liu, and Y. S. Ang, Ferroelastic altermagnetism, arXiv: 2505.20843 (2025)
116. S. Wang, W. W. Wang, J. Fan, X. Zhou, X. P. Li, and L. Wang, Two-dimensional dual-switchable ferroelectric altermagnets: Altering electrons and magnons, *Nano Lett.* 25(40), 14618 (2025)
117. T. Wang, J. Li, B. Wang, and H. Jin, PU-learning-guided discovery of synthesizable multiferroic nitride perovskites with altermagnetic order, *npj Comput. Mater.*, doi: 10.1038/s41524-025-01876-z (2025)
118. I. Khan, D. Bezzerga, and J. Hong, Coexistence of altermagnetism and robust ferroelectricity in a bulk

MnO Wurtzite structure, *Mater. Horiz.* 12(7), 2319 (2025)
119. S. Wu, P. Diao, W. Sun, C. Yang, S. Huang, and Z. Cheng, Band-rearrangement-enabled nonvolatile altermagnetism switching in 2D ferroelectric/magnetic heterostructures, *Adv. Funct. Mater.*, doi: 10.1002/adfm.202516174 (2025)
120. W. Z. Xiao, Janus Mn_2OS monolayers with piezoelectric altermagnetism and their application in photocatalytic water splitting, *New J. Chem.* 50(1), 424 (2026)
121. Y. Yang, K. Zou, G. Wang, D. Y. Liu, L. J. Zou, F. Lu, and W. H. Wang, Enhanced altermagnetic splitting through modulating altermagnetic–ferroelectric coupling in monolayer multiferroic Ti_2S_2O, *Appl. Phys. Lett.* 127(7), 072903 (2025)
122. D. Bezzerga, I. Khan, and J. Hong, High performance room temperature multiferroic properties of w-MnSe altermagnet, *Adv. Funct. Mater.* 35(43), 2505813 (2025)
123. X. Yang, S. S. Wang, and S. Dong, A large spin-splitting altermagnet designed from the hydroxylated MBene monolayer, *Adv. Funct. Mater.*, doi: 10.1002/adfm.202517921 (2025)
124. N. Ding, H. Ye, S. S. Wang, and S. Dong, Ferroelasticity tunable altermagnets, arXiv: 2510.14193 (2025)
125. R. He, D. Wang, N. Luo, J. Zeng, K. Q. Chen, and L. M. Tang, Nonrelativistic spin-momentum coupling in antiferromagnetic twisted bilayers, *Phys. Rev. Lett.* 130(4), 046401 (2023)
126. Y. Liu, J. Yu, and C. C. Liu, Twisted magnetic van der Waals bilayers: An ideal platform for altermagnetism, *Phys. Rev. Lett.* 133(20), 206702 (2024)
127. Y. Sheng, J. Zhang, J. Liu, and M. Wu, Ubiquitous van der Waals altermagnetism with sliding/moiré ferroelectricity, *Sci. China Phys. Mech. Astron.* 68(9), 297511 (2025)
128. S. Sheoran and S. Bhattacharya, Nonrelativistic spin splittings and altermagnetism in twisted bilayers of centrosymmetric antiferromagnets, *Phys. Rev. Mater.* 8(5), L051401 (2024)
129. Z. Gao, F. Ma, T. He, X. Zhang, Y. Liu, A. Du, and Y. Jiao, Ultrafast laser-induced demagnetization and valley polarization in a room-temperature altermagnetic Cr_2MoS_4 monolayer, *J. Phys. Chem. Lett.* 16(49), 12561 (2025)
130. H. Chen, F. Chen, H. Cheng, X. Zhao, G. Hu, X. Yuan, and J. Ren, Layer-locked multiple valley Hall effects in tetragonal altermagnetic/ferromagnetic monolayers M_2SiCX_2 (M=transition metal; X=S, Se), *Phys. Rev. B* 111(15), 155428 (2025)
131. Y. Wu, L. Deng, X. Yin, J. Tong, F. Tian, and X. Zhang, Valley-related multipiezo effect and noncollinear spin current in an altermagnet Fe_2Se_2O monolayer, *Nano Lett.* 24(34), 10534 (2024)
132. Y. Q. Li, Y. K. Zhang, X. L. Lu, Y. P. Shao, Z. Q. Bao, J. D. Zheng, W. Y. Tong, and C. G. Duan, Ferrovalley physics in stacked bilayer altermagnetic systems, *Nano Lett.* 25(15), 6032 (2025)
133. N. J. Yang, Z. Huang, and J. M. Zhang, Spin-selective second-order topological insulators enabling cornertronics in two-dimensional altermagnets, *Nano Lett.* 25(43), 15495 (2025)
134. X. Chen, D. Wang, L. Li, and B. Sanyal, Giant spin-splitting and tunable spin-momentum locked transport in room temperature collinear antiferromagnetic semimetallic CrO monolayer, *Appl. Phys. Lett.* 123(2), 022402 (2023)
135. H. Shi, Y. Jiang, Y. Tian, W. Wang, S. Li, W. J. Gong, and X. Kong, Tunable quantum layer spin Hall effect in bilayer altermagnetic Nb_2SeTeO, *Appl. Phys. Lett.* 128(6), 063101 (2026)
136. Y. Wu, L. Deng, X. Yin, J. Tong, F. Tian, and X. Zhang, Valley-related multipiezo effect and noncollinear spin current in an altermagnet Fe_2Se_2O monolayer, *Nano Lett.* 24(34), 10534 (2024)
137. H. Y. Ma, D. Guan, S. Wang, Y. Li, C. Liu, H. Zheng, and J. F. Jia, Quantum spin Hall and quantum anomalous Hall states in magnetic Ti_2Te_2O single layer, *J. Phys.: Condens. Matter* 33(21), 21LT01 (2021)
138. S. D. Guo, X. S. Guo, K. Cheng, K. Wang, and Y. S. Ang, Piezoelectric altermagnetism and spin-valley polarization in Janus monolayer Cr_2SO, *Appl. Phys. Lett.* 123(8), 082401 (2023)
139. S. Singh, P. C. Rout, M. Ghadiyali, and U. V. Schwingenschlögl, $_2Se_2O$ and Janus V_2SeTeO: Monolayer altermagnets for the thermoelectric recovery of low-temperature waste heat, *Mater. Sci. Eng. Rep.* 166, 101017 (2025)
140. C. Chen, X. He, Q. Xiong, C. Quan, H. Hou, S. Ji, J. Yang, and X. Li, Strain-modulated valley polarization and piezomagnetic effects in altermagnetic Cr_2S_2, *Appl. Phys. Lett.* 127(10), 102409 (2025)
141. W. Zhang, E. Zhu, Z. Li, and H. Lv, Strain-tunable spin-valley locking and the influence of spin–orbit coupling in the two-dimensional altermagnet V_2Te_2O, *Phys. Rev. B* 112(14), 144427 (2025)
142. J. Sun, Y. Du, and E. Kan, Symmetry-breaking magneto-optical effects in altermagnets, *Nano Lett.* 25(41), 14960 (2025)
143. Y. Chang, Y. Wu, L. Deng, X. Yin, and X. Zhang, Valley-related multipiezo effect in altermagnet monolayer V_2STeO, *Materials (Basel)* 18(3), 527 (2025)
144. I. Khan, D. Bezzerga, B. Marfoua, and J. Hong, Altermagnetism, piezovalley, and ferroelectricity in two-dimensional Cr_2SeO altermagnet, *npj 2D Mater. Appl.* 9(1), 18 (2025)
145. J. Gong, Y. Wang, Y. Han, Z. Cheng, X. Wang, Z. M. Yu, and Y. Yao, Hidden real topology and unusual magnetoelectric responses in two-dimensional antiferromagnets, *Adv. Mater.* 36(29), 2402232 (2024)
146. X. Zou, X. Feng, Y. Dai, B. Huang, and C. Niu, Floquet quantum anomalous Hall effect with in-plane magnetization in two-dimensional altermagnets, *ACS Nano* 19(40), 35575 (2025)
147. J. Y. Li, A. D. Fan, S. Li, and W. L. Yang, Optical dichroism, valley polarization, and noncollinear spin currents in monolayer altermagnetic $Ca(CoN)_2$, *Appl. Phys. Lett.* 127(13), 131901 (2025)
148. Z. Zhang, H. Sun, M. Dong, Y. Guo, and M. Zhao, Giant valley splitting and tunable anisotropic spin plasmons in a Janus ferrovalley monolayer, *npj*

Comput. Mater. 11(1), 277 (2025)

149. Q. Wang, L. Deng, Y. Wu, J. Tong, X. Yin, and X. Zhang, Achieving large valley polarization in altermagnet semiconductor $Mg(FeN)_2$ monolayer, *Inorg. Chem.* 64(35), 17785 (2025)
150. W. Xun, X. Liu, Y. Zhang, Y. Z. Wu, and P. Li, Stacking-, strain-engineering induced altermagnetism, multipiezo effect, and topological state in two-dimensional materials, *Appl. Phys. Lett.* 126(16), 161903 (2025)
151. H. Zeng, W. Zhang, C. Qiu, D. Z. Ding, and J. Zhao, Symmetry breaking induced nonrelativistic spin splitting and spontaneous valley polarization in altermagnetic $Ca(CoN)_2$ bilayer, *Appl. Phys. Lett.* 126(20), 202405 (2025)
152. W. Sun, W. Wang, C. Yang, R. Hu, S. Yan, S. Huang, and Z. Cheng, Altermagnetism induced by sliding ferroelectricity via lattice symmetry-mediated magnetoelectric coupling, *Nano Lett.* 24(36), 11179 (2024)
153. Y. Wei, X. Li, H. Wang, Y. Wang, T. Cao, and X. Fan, The switchable quantum anomalous Hall effect and altermagnetism in Janus monolayer and bilayer $V_2WS_2Se_2$, *J. Mater. Chem. C* 13(42), 21498 (2025)
154. Y. Qi, J. Zhao, and H. Zeng, Spin-layer coupling in two-dimensional altermagnetic bilayers with tunable spin and valley splitting properties, *Phys. Rev. B* 110(1), 014442 (2024)
155. S. D. Guo, X. S. Guo, and G. Wang, Valley polarization in two-dimensional tetragonal altermagnetism, *Phys. Rev. B* 110(18), 184408 (2024)
156. S. D. Guo, Y. Liu, J. Yu, and C. C. Liu, Valley polarization in twisted altermagnetism, *Phys. Rev. B* 110(22), L220402 (2024)
157. S. D. Guo, Valley polarization in two-dimensional zero-net-magnetization magnets, *Appl. Phys. Lett.* 126(8), 080502 (2025)
158. Z. Zhu, R. Huang, X. Chen, X. Duan, J. Zhang, I. Zutic, and T. Zhou, Altermagnetic proximity effect, arXiv: 2509.06790 (2025)
159. W. Xie, L. Wang, X. Xu, Y. Yue, H. Xia, L. He, and H. Wang, Realizing giant valley polarization effect based on monolayer altermagnets, *Acta Phys. Sin.* 74(22), 227501 (2025)
160. L. Zhang, Y. Liu, J. Ren, G. Ding, X. Wang, G. Ni, G. Gao, and Z. Cheng, Lithium and vanadium intercalation into bilayer V_2Se_2O: Ferrimagnetic–ferroelastic multiferroics and anomalous and spin transport, *Adv. Sci.*, doi: 10.1002/advs.202512533 (2025)
161. X. Sun, X. Yu, S. D. Guo, and S. Chen, Strain-induced altermagnetism to ferromagnetism transition in monolayer $Cr_2Si_2S_3Se_3$, *J. Phys.: Condens. Matter* 37(44), 445801 (2025)
162. A. Zaman, K. Husain, S. H. Alrefaee, H. Shahid, M. Elhadi, A. Nurmuhammedov, R. M. Mohammed, V. Tirth, A. Algahtani, and N. Elboughdiri, Multipiezo effect in altermagnet V_2SeO monolayer at high temperature, *Case Stud. Therm. Eng.* 74, 106943 (2025)
163. B. Jiang, M. Hu, J. Bai, Z. Song, C. Mu, G. Qu, W. Li, W. Zhu, H. Pi, Z. Wei, Y. J. Sun, Y. Huang, X. Zheng, Y. Peng, L. He, S. Li, J. Luo, Z. Li, G. Chen, H. Li, H. Weng, and T. Qian, A metallic room-temperature d-wave altermagnet, *Nat. Phys.* 21(5), 754 (2025)